STUDY OF SG IRON AND ITS TRIBOLOGICAL BEHAVIOUR

A THESIS SUBMITTED IN PARTIAL FULFILMENT
OF THE REQUIREMENTS FOR THE DEGREE OF

Master of Technology

In

Metallurgical and Materials Engineering

By

RELIANCE JAIN

Department of Metallurgical and Materials Engineering

National Institute of Technology

Rourkela 2013

STUDY OF SG IRON AND ITS TRIBOLOGICAL BEHAVIOUR

A THESIS SUBMITTED IN PARTIAL FULFILMENT
OF THE REQUIREMENTS FOR THE DEGREE OF

Master of Technology

In

Metallurgical and Materials Engineering

By

RELIANCE JAIN

Under the Guidance of

Prof. S. SEN
&
Prof. S. C. MISHRA

Department of Metallurgical and Materials Engineering

National Institute of Technology

Rourkela 2013

National Institute of Technology
Rourkela

CERTIFICATE

This is to certify that thesis entitled, "STUDY OF SG IRON AND ITS TRIBOLOGICAL BEHAVIOUR" submitted by Mr. Reliance Jain in partial fulfillment of the requirements for the award of Master of Technology Degree in Metallurgical and Materials Engineering at National Institute of Technology, Rourkela (Deemed University) is an authentic work carried out by him under our supervision and guidance.

To the best of our knowledge, the matter embodied in this thesis has not been submitted to any other university/ institute for award of any Degree or Diploma.

Prof. S.C.Mishra

Date:

Dept. of Metallurgical and Materials Engineering

National Institute of Technology

Rourkela-769008

Prof. S.Sen

Date:

Dept. of Metallurgical and Materials Engineering

National Institute of Technology

Rourkela-769008

ACKNOWLEDGEMENT

I avail this opportunity to extend my hearty indebtedness to my guide **Prof. S. Sen & Prof. S. C. Mishra, Dept. of Metallurgical and Materials Engineering, NIT, Rourkela** for their invaluable guidance, motivation, untiring efforts and meticulous attention at all stages during my course of work.

I express my sincere thanks to Prof. B. C. Ray, Head of the Department of Metallurgical and Materials Engineering, NIT, Rourkela for providing me the necessary facilities in the department. I am also grateful to Prof. Krishna Datta M. Tech. co-coordinator, for his constant concern and encouragement for execution of this work.

I also express my sincere gratitude to **Prof. S. K. Acharya**, **Dept. of Mechanical Engineering** for his timely help during the course of work.

I thankful to Sri Rajesh Pattnaik, Sri Hembram & Sri Udayanath Sahu, Metallurgical & Materials Engineering, Technical assistants, for their co-operation in experimental work.

DATE:

RELIANCE JAIN

ROLL NO. 211MM1360

CONTENTS

ABSTRACT

Erosive wear tests were performed on different alloys composition of SG iron using air jet erosion test rig. Erosion damage was measured by the removed material volume at impact angles 30˚, 45˚ and 60˚. The effect of impact angle, standoff distance and pressure in wear features of specimens were discussed as mechanism of erosive wear by using the taguchi's analysis. The objective was to investigate which design parameter significantly affects the erosion wear. It was found that the pressure and impact angle is the most powerful factor influencing the erosion wear rate.

The surface morphology shows erosion mechanism of the spheroidal graphite at the surface deforms gradually, lips are produced in the direction of the blast, and they extend, and finally drop off. This process of growth, extension, and dropping off is repeated, but life spans are different depending on the material**.** The basic mechanism of the erosion damage is at first the plastic transformation near the surface due to the impacts. In this study we deal with determination of crystallite-size distribution and microstrain measurement of SG iron by the means of x-ray diffraction line broadening method. XRD analysis shows that only ferrite phase is present mainly in all samples of SG iron. It was shown that nodular cast iron has excellent erosion resistance and it is expected to find wide applications as a wear-resistant material. Nodular cast iron (SG iron) shows the highest wear resistance probably due to its graphite morphology which controls crack propagation and thermal conductivity.

LIST OF FIGURES

LIST OF TABLES

CHAPTER 1

INTRODUCTION

- Background
- Objectives of the present piece of investigation

1.1 Background

Ductile iron or spheroidal graphite cast irons, which have been developing over the past few decades, are of considerable current attention because they can proposal a better combination of strength and toughness as compared with gray cast irons. Such a necessary combination of mechanical properties of ductile iron coupled with the intrinsic cost advantage of the casting process has resulted in an increased use of ductile iron in recent years, even replacing fabricated steel components in some cases. Austempered Ductile Iron (ADI) is described by improved mechanical properties but low machinability compared to conventional ductile iron materials and steels of same strengths. The mechanical properties of ADI are achieved by a very fine austenitic-ferritic microstructure.

Nodular cast iron is a heterogeneous material. The macroscopic properties of this material have been often measured using a traction test **[1].** Nevertheless, the microscopic study showed that destruction is produced by the plastic cavitation and the uncertainty of the ductile matrix surrounding the graphitic spheroids that act like a wide cavity. Severe damage can be produced by the growth of the cavitation that surrounds the presences in the ferretic phase **[2].**

Ductile Iron also referred to as nodular iron or spheroidal graphite iron was patented in 1948.After a decade of intensive development work in the 1950s, ductile iron had a phenomenal increase in use as engineering material during 1960s, and the rapid increase in commercial application continues today.

Ductile iron as a technologically valued material has been employed for a score of years during this period while many investigators have inspected its mechanical performance under a wide range of situations others have attempted to explain its solidification behavior and the many variables which interfere in producing an acceptable product. However even at this date we are still at a loss to explain in a fundamental way how an otherwise flake like graphite shape develops in to the spheroidal morphology which gives ductile iron its superior properties.

Fig1 represents the meso-scale of the nodular cast iron. It shows that the material comprises three phases: ferrite (white), pearlite (grey) and graphitic spheroid (black). In this case the matrix can be considered by way of formed by two constituents: ferrite and pearlite. Furthermore, tribological behavior of nodular cast iron depends, on one hand, on the different individual constituent properties and their interactions and on the other hand on the tribological parameter system **[3-5].** Generally, the micro-mechanical models have been used to appreciate the local mechanisms which govern the elastic and plastic deformation of a heterogeneous material. It supplies the global response of the heterogeneous material using different properties of every individual constituent and their interactions **[6].**

All ferrous materials other than those having an austenitic matrix may fail in a ductile or a brittle manner according to the method of testing and the geometry of the test piece, the temperature of testing, the structure and the composition of the material **[7-9].** The randomly oriented crystals or grains of metal undergo plastic deformation by a process of slip which is due to a shear stress caused by the lamellae of the crystal sliding over one another **[10-11].** Failure by slip only occurs after a large amount of plastic deformation and will be accompanied by a considerable elongation of the test piece in a tensile test. Besides, crystals sometimes fail by cleavage due to separation on a plane known as a cleavage plane. Such failure is of a sudden brittle nature and occurs when the tensile stress, Normal to the cleavage plane, exceeds the cohesive strength of the material.

In a tensile test, when a crack is first initiated, there is a considerable amount of elastic energy stored in the specimen, as a large volume of material is stressed to the maximum stress level. This energy is released when failure starts and serves to propagate the crack. The release of elastic energy speeds up crack propagation, and depending on the chemical composition, a certain speed may be exceeded causing the fracture to change from ductile state to brittle state.

The first commercial applications of Austempered Ductile Iron (ADI) occurred in 1972. But, the history of the development of ADI spans from the 1930's to the present. Revolutionary heat treatment work with steel (1930's) and the discovery of ductile cast iron (1940's) are included among the important events which lead to the development of ADI.

In the 1930's, work was conducted by Bain et al on the isothermal transformation of steel. A new micro constituent was discovered that was described as "an acicular, dark etching aggregate." This new microstructure exhibited promising properties as it was found to be tougher, for the same hardness, than tempered martensite **[12].**

In the 1940's Keith Millis was assigned the task of examining elements to additional for chromium in the production of Ni Hard cast iron at the International Nickel Company (INCO). This study eventually leads to the treatment of gray cast iron with magnesium. On examination, spheroidal shaped graphite was found in this cast iron. The first magnesium treated ductile iron had been produced.

Tribology is the science and technology of interrelating surfaces in relative motion. Tribology includes boundary-layer interactions both between solids and between solids and liquids and/or gases. Tribology aims to optimize friction and wear for a specific application case. Apart from satisfying the required function, this means promising high efficiency and sufficient reliability at the lowest possible manufacturing, assembly, and maintenance costs.

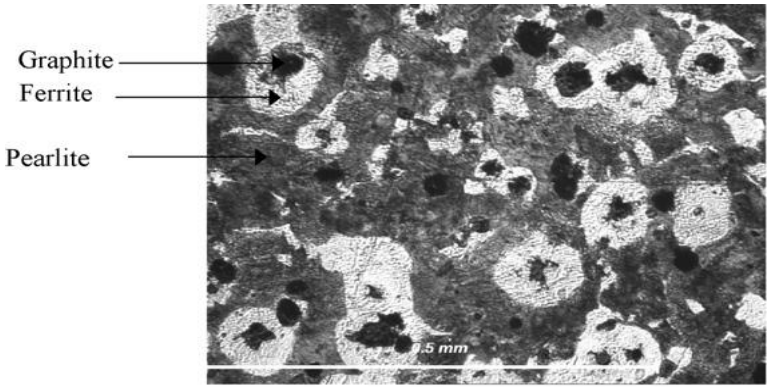

Fig. 1. Meso scale structure of a nodular cast iron.

Wear be present one of the greatest commonly encountered industrial problems, leading to common replacement of components, particularly abrasion. Wear resistance, is not an intrinsic property of the material but also depends upon the tribological behavior, such as properties of materials tested, erodent grit size, test condition (temperature and pressure), equipment, and

atmosphere **[13–15].** In order to achieve optimal wear properties, an accurate forecast of wear of ADI's is essential. Hence, numerous mathematical models based on statistical regression techniques have been constructed to select the proper testing conditions **[16–19].** The Taguchi's design can be further simplified by expanding the application of the traditional experimental design to the use of orthogonal array.

Most of the study has been dedicated on the experimental work of dry wear behavior of ductile iron, cast iron, compact graphite iron and ADI's **[20–26].** Though, a few research works have been conducted on the abrasive wear of ADI sample **[27–32].** Moreover, no efforts have so far been made to optimize the wear resistance of ADI using a statistical analysis. The aim of the present study is, therefore, to investigate the wear behavior of ADI samples with different composition based on the Taguchi method under various testing conditions. Furthermore, the analysis of variance is employed to examine the testing characteristics of ADI's with different composition.

Erosion wear rate not only be subject to on the mass flow, impact angle and velocity of the erodent, also depends on the spraying parameters. Only the spraying process is dependent on around 150 factors, hence we cannot account all the factors during the experiment. To account all the factors, Prediction of erosion wear rate properties by some numerical technique is one of the most important requirements. Artificial neural networks have the ability to tackle the problem of complex relationships between variables that cannot be accomplished by more traditional methods. Simple linear regression is not an answer for process like these that have nonlinear properties. Another advantage of using ANN model is that it can predict an output with accuracy even if the variable interactions are not wholly understood. Artificial neural networks (ANN), which is a method that involves, database exercise to forecast property-parameter evolutions. This section presents the database creation, implementation protocol and a set of expected results related to the erosion wear rate. The details of this approach are defined by Rajasekaran and Pai **[33].**

Erosive wear, or the sand erosion phenomenon, has been a serious problem in many industrial systems since last century. Recently, big accidents have occurred due to the erosive

wear phenomena. Take the pipe damage in the Mihama power station for example; the wall of pipe in the factory was thinned down by erosive–corrosive wear, resulting in the accident. Similarly, the erosion phenomena can cause serious problems; mainly at bended sections of pipe, valve, turbine blade, the fan in a pneumatic conveying system, and even the blade of helicopter, etc. **[1–5]** may be damaged. Instances of sand erosion occur in secondary refining and smelting reduction equipment at iron and steel plants. When the dispersed particles such as dust coal, powdered mineral, etc. were blown into the melted pig iron through blowpipes, the erosion damage occurred at the bended section of the pipe. If these kinds of pipe systems were eroded and were perforated in places by gas entrained particles that penetrate the inner surface, they would likely result in causing serious industrial accidents.

Mechanism of erosive wear in pipe was very complex, and there occurred a large amount of damages by erosive wear. Nevertheless, it could not predict which part in the pipe was most damaged and how much life span the pipe had left. So when regular maintenance was performed, the inner wall of the pipe to be thinned down was built up through welding in order to avoid causing accidents. But this kind of prevention is only temporary; damage will occur again in 2–3 weeks. Therefore, to further prevent the accident from occurring, important research is being done about the development of wear-resistant material and estimation of life span during erosion.

1.2 OBJECTIVES OF THE PRESENT PIECE OF INVESTIGATION

The objectives of the present piece of investigation are as follows:

• To study of erodent properties on erosion wear of ductile type materials (SG iron).

• To Study of microstructural evolution and mechanical properties SG iron.

• To Study of different composition in spheroidal graphite cast iron and its effect on wear rate.

• X-ray diffraction studies for phase analysis.

• To investigate the erosion behavior of SG iron based on the Taguchi method under various testing conditions.

• ANN computational technique (Artificial neural network analysis) is used to forecast the erosion wear rate under different working conditions.

.

• Analysis of variance (ANOVA) is employed to investigate the most significant control factors and their interactions. Finally, an evolutionary approach known as genetic algorithm has been applied for optimal factor settings to minimize the erosion rate.

• To analysis the experimental results using statistical techniques and find out the significant factors/interactions affecting the erosion wear rate.

.

CHAPTER 2

LITERATURE SURVEY

- Preamble
- A Brief Discussion about Ductile Iron
- Factors that affect Properties of Ductile Iron
- Mechanical Properties of Ductile iron
- A Taguchi and ANOVA approach for investigation of wear
- Application of SG iron in Automotive Industry
- Wear
- Types of wear
- Symptoms of wear
- Recent trends in metal wear research
- ANN method
- Erosive wear characteristics of spheroidal carbides cast iron

2.1 Preamble

In this chapter we deal with the literature survey of the broad topic of interest namely the tribological behavior of austempered ductile iron (SG iron). It also deals with A Brief Discussion about Ductile Iron, Factors that affect Properties of Ductile Iron, Mechanical Properties of Ductile iron, A Taguchi and ANOVA approach for investigation of wear and Application of SG iron in Automotive Industry. This chapter also deals with an assessment of the wear, types of wear, symptoms of wear and recent trends in metal wear research along with erosion wear behavior of SG iron which is the material of interest in this work.

At the end of the chapter a brief discussion of the literature survey and the knowledge gap in the previous investigations are presented..

2.2 A Brief Discussion about Ductile Iron

Ductile iron is defined as a high carbon containing, iron based alloy in which the graphite exists in compact, spherical shapes rather than in the shape of flakes, the latter being typical of gray cast iron. As ductile iron, occasionally referred to as nodular or spheroidal graphite cast iron, constitutes a family of cast irons in which the graphite is present in a nodular or spheroidal form. The graphite nodules are small and constitute only small areas of weakness in a steel-like matrix. Because of this the mechanical properties of ductile irons associated directly to the strength and ductility of the matrix present—as is the case of steels.

The graphite occupies about 10-15% of the total material volume and because graphite has small tensile strength, the main effect of its presence is to reduce the effective cross-sectional area, which means that ductile iron has tensile strength, modulus of elasticity and impact strength proportionally lower than that of a carbon steel of otherwise alike matrix structure.

The matrix of ductile irons can be varied from a soft and ductile ferritic structure, through harder and higher strength pearlitic structures to a hard, higher and comparatively tough tempered martensitic or bainitic structure. Thus, a wide range of combinations of strength and ductility can be achieved. General engineering grades of ductile iron commonly have the structures which are ferritic or ferrito-pearlitic. Well-ordered processing of the molten iron

precipitates graphite as spheroids rather than flakes. The round shape of the graphite eliminates the material's tendency to crack and helps prevent cracks from spreading.

2.2.1 Chemical Composition

Chemically this material is same as grey iron and is Fe-C-Si alloy. It is one of the more recent developments in cast iron technology has been around since 1948. As the name suggests, it was established to overcome the brittle nature of grey and white irons. It is also quite ductile in as cast form. The main trace elements present in ductile iron can have a noticeable influence on the structure and hence the properties of the iron. With the exception of silicon, all elements encourage pearlite and all elements with the exception of silicon, nickel and copper also encourages carbides. The strength properties of ferritic ductile iron are generally increased by the elements, which go in to the solution. With the exception of carbon, all the elements increase tensile strength and hardness. An example of the extent to which ferrite is affected by solid solution strengthening is demonstrated for the elements silicon and nickel. 1% addition of silicon raises the proof and tensile strength of a ferritic iron by approximately 82 N/mm_2 whereas 1% of nickel increases these properties by 46 N/mm_2. In the ferritic irons increase in tensile strength and proof strength are obtained at the expense of ductility and in such case the iron can become embrittled.

2.2.2 Structure

The main difference between ductile iron and grey iron is the morphology of graphite particles which take on a nodular or almost spherical form after appropriate treatments are made to the melt. The chief microstructural constituents of ductile iron are: the chemical and morphological forms taken by carbon, and the continuous metal matrix in which the carbon and/or carbide are dispersed. The following significant microstructural components are found in ductile iron.

- Graphite

This is the stable form of pure carbon in cast iron. Its important physical properties are low density, low hardness and high thermal conductivity and lubricity. Graphite shape, which

can range from flake to spherical, plays an important role in determining the mechanical properties of ductile irons. Ductile iron is categorized by having all of its graphite occurs in microscopic spheroids. Even though this graphite constitutes about 10% by volume of ductile iron, its compact spherical shape minimizes the effect on mechanical properties. The graphite in commercially produced ductile iron is not always in perfect spheres.

- Ferrite

This is the purest iron phase in a cast iron. In conventional Ductile Iron ferrite produces lower strength and hardness, but high ductility and toughness. In Austempered Ductile Iron (ADI), enormously fine grained acicular ferrite provides an excellent combination of high strength with good ductility and toughness. The strength properties of ferritic ductile iron are generally increased by the elements, which go in to the solution.

- Pearlite

Pearlite, produced by a eutectoid reaction, is a close mixture of lamellar cementite in a matrix of ferrite. It is common constituent of cast irons; pearlite gives a mixture of higher strength and with a corresponding reduction in ductility which meets the requirements of many engineering applications.

- Martensite

Martensite is a supersaturated solid solution of carbon in iron formed by rapid quenching. Due to very high lattice distortion it is very brittle and hard. Martensite is produce by shear deformation process.

- Austenite

Normally a high temperature phase containing of carbon dissolved in iron, it can be present at room temperature in austenitic and austempered cast iron. In austenitic irons, austenite is stabilized by nickel in the range of 18-36% **[34].** It is also known as gamma iron, it is produced by a combination of rapid cooling which suppress the formation of pearlite and the supersaturation of carbon during austempering process, which reduce the start of the austenite-to-martensite transformation far below room temperature.

In austenitic irons, the austenite matrix offers ductility and toughness at all temperatures, corrosion resistance and good high temperature properties, especially under thermal cycling conditions. In austempered ductile iron stabilized austenite, in volume fractions

up to 40% in lesser strength grades, advances toughness and ductility and response to surface treatments such as fillet rolling.

- Bainite

The mechanism of transformation austenite to bainite is complicated and controversial. It is acicular microstructure which produces in temperature range 250˚C to 550 ˚C.

2.2.3 Family of Ductile Iron

Through a high percentage of graphite nodules present in the structure, mechanical properties are determined by the ductile iron matrix. The importance of matrix in controlling mechanical properties is give importance to by the use of matrix names to designate the following types of Ductile Iron.

- Ferritic Ductile Iron

Graphite spheroids in a matrix of ferrite provide an iron with good ductility and impact resistance and with a tensile and yield strength same to low carbon steel.

- Ferrito- Pearlitic Ductile Iron

These are the most common rating of ductile iron and are normally produced in the as-cast condition.

- Pearlitic Ductile Iron

Graphite spheroids in a matrix of pearlite result in an iron with high strength, good wear resistance, and modest ductility and impact resistant. Machinability is also more to steels of equivalent physical properties.

- Austempered Ductile iron (ADI)

ADI, the latest addition to the ductile iron family, is a sub-group of ductile iron produced by giving conventional ductile iron a special austempering heat treatment. Closely twice as strong as pearlitic ductile iron, ADI still retains high elongation and toughness. This combination delivers a material with more wear resistance and fatigue strength.

2.3 Factors that affect Properties of Ductile Iron

Ductile iron is a special kind of material which shows a good combination of strength with ductility confirming its huge application in heavy engineering industries. This is due to very characteristic microstructure due to its chemical composition, heat treatment practice and processing variables. Some lists of important constituents which are responsible for its typical mechanical properties are below.

- Graphite Shape
- Carbide in the Structure
- Nodule Count
- Graphite Volume
- Matrix

  In Ductile Irons with consistent nodularity and nodule count and small porosity and carbide content, mechanical properties are determined generally by the matrix constituents and their hardness.

- Temperature on Design stress
- Environment on Tensile Properties
- Metal Cleanliness
- Composition- The magnetic, electrical and thermal properties of ductile irons are influenced by the composition of the matrix present in ductile iron. Composition of ductile iron very important for defining its mechanical, thermal and electrical properties.

2.4 Mechanical Properties of Ductile iron

The several, successful uses of ductile iron in critical components in all sectors of industry highlight its flexibility and suggest many supplementary applications. In order to use ductile iron with assurance, the design engineer must have admittance to engineering data describing the following mechanical properties: elastic properties, strength, ductility, hardness, fracture toughness and fatigue properties. Physical properties like thermal expansion, thermal conductivity, heat capacity, density, and magnetic and electrical properties are also of attention

in many applications. This Section describes the mechanical and physical properties of conventional Ductile Irons, relates them to microstructure, and indicates how composition and further production parameters affect properties through their influence on microstructure.

- Tensile Properties

The tensile properties of conventional Ductile Iron, particularly the yield and tensile strengths and elongation, have conventionally been the most widely mentioned and applied determinants of mechanical behavior. Poisson's Ratio, the ratio of lateral elastic strain to longitudinal elastic strain produced during a tensile test, shows little deviation in Ductile Iron.

- Elongation

Elongation is defined as the permanent increase in length, expressed as a percentage of a specified gage length marked in a tensile test bar, which is formed when the bar is tested to failure. Elongation is used usually as the primary indication of tensile ductility and is included in many Ductile Iron specifications.

- Hardness

The hardness of Ductile Iron is typically and best measured by the Brinell test, in which a 10 mm diameter hardened steel or tungsten carbide ball is pressed into a flat surface of the work piece. Hardness is expressed as a Brinell Indentation Diameter (BID) or a Brinell Hardness Number (BHN). Brinell hardness should be used for production control and as an auxiliary property test, for example to control machinability. Microhardness testing, using either the Knoop or Vickers hardness indenters, can be used to measure the hardness of the separate components of the Ductile Iron matrix.

- Machinability

Machinability is a very important property of any material and this is generally depends upon operating condition, various cutting devices functioned at different rates under different lubricating condition. Traditionally, machinability has been measured by determining the correlation between cutting speed and tool life because these factors directly impact machine tool productivity and machining costs.

- Effect of Microstructure

Machinability is determined by microstructure and hardness. The graphite particles in ductile iron are accountable for the free-machining characteristics of this material and its greater machinability when compared to steels. Graphite particles influence cutting force and surface finish, the matrix is the primary determinant of tool life and Ferrite is the softest constituent in the matrix of ductile iron and as a result shows the best machinability.

Pearlite, which consists of an intimate mixture of soft ferrite and hard lamellar iron carbide, is a common matrix component in all in-between strength grades of ductile iron. The volume fraction of pearlite and fineness of the lamellar determine the hardness and the machinability and wear resistance. Pearlite fineness affects machinability and the effect of hardness decreases as pearlite fineness increases and Carbides are the hardest constituents in the ductile iron and have the poorest machinability.

2.5 Application of SG iron in Automotive Industry

After the ground breaking application of ADI to compressor crankshafts by Tecumseh products in 1972, a flurry of engineering activity was undertaken. In those early years the process was not well quantified and ADI was met with only mixed success. However, in a project originally started in the 1960's, GM was methodically developing an ADI gear program.

Meanwhile, in Europe, the Jot Companies had begun coordinating ADI developments for truck applications. By working with Oy Sis-Auto Ab (Finland), they developed a differential spider (Fig.2.1) that replaced carburized steel. Meehanite Metal Corp. **[35]** indicated that the manufacturing process was cut from ten steps to two. In-service testing of these components showed a measurable decrease in wear due to the improved sliding properties of ADI-to-steel as compared to steel to-steel.

Fig. 2.1- ADI differential cross (spider)

In the 1980's GM first applied ADI for an engine component. They selected the camshaft for the L -4 engine. This camshaft was produced for GM by Intermet Corporation and exceeded the requirement of 250ksi (1,750 MPa) contact stress at ten million cycles with no pitting. This camshaft was employed for the production life of the L-4 engine. Soon ADI production in North America began to outstrip production in Europe and Asia combined. North American auto producers were no exception, employing ADI for engine brackets at GM, Ford and Mazda (Fig.2.2).

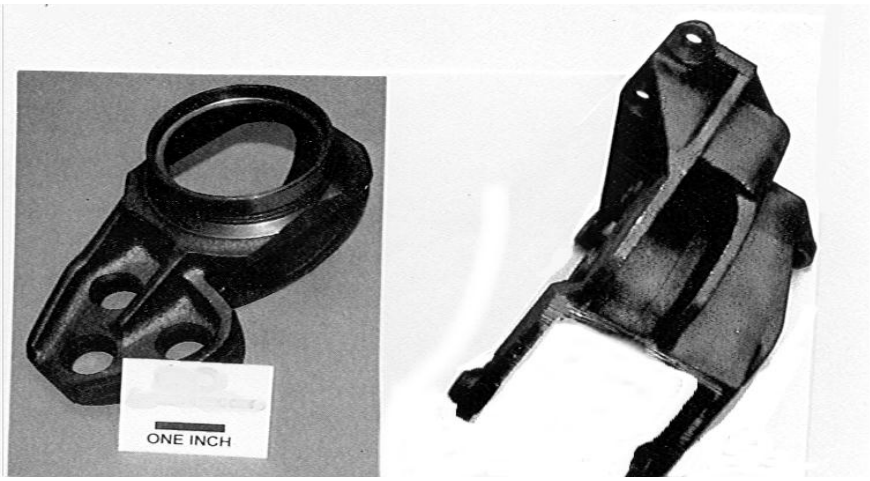

Fig. 2.2 – (a) Ford / Mazda engine bracket, (b) Ford Taurus SH engine bracket.

By 1984 Cummins had employed ADI timing gears in its series B and C diesel engines (Fig2.3). These gears, produced by Getrag, were produced using virtually the same process created by GM for the hypoid ring and pinion gear sets in 1977. Though the process has gone through some modifications, Cummins is still a volume user of ADI timing gears for its diesel

engines. Trac-Tech found ADI to be the perfect component material for their popular Detroit Locker differential (Figure 2.4)**.**

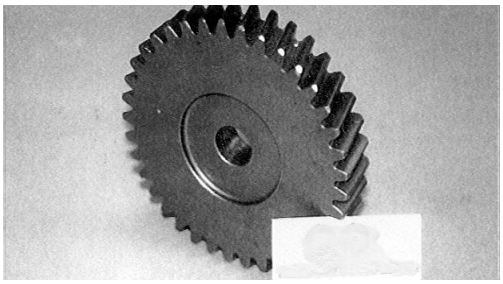

Fig.2.3 -ADI timing gear for a Cummins diesel engine.

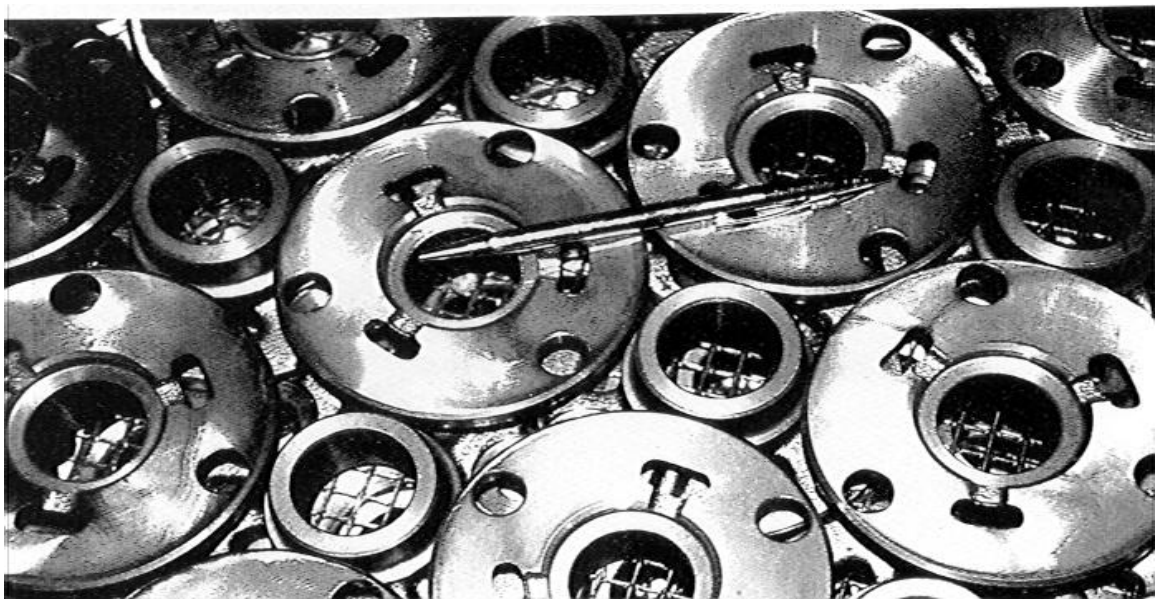

Fig.2.4 - ADI differential case covers.

By the mid-1990 the Motor Industry Research Association (MIRA) had finished work on an ADI crankshaft development program **[36].** That program produced the proper material, process and design characteristics necessary for a successful ADI crankshaft implementation except for one tiny detail.

By the 1990's Navistar, Freightliner, Kenworth, GM, Iveco, Volvo and other heavy truck manufacturers had adopted ADI as a high performance, low cost material for spring hanger brackets and U-bolt brackets, accessory brackets, and shock absorber brackets (Fig. 2.5). North American as well as various European suppliers had adopted ADI for brake spiders (Fig. 2.6), steering knuckles (Fig. 2.7) and steering arms (Fig.2.8)

In some automotive circles, cast iron has been "given up for dead". For now the average amount of ductile iron per vehicle is increasing and ADI is being found in new applications throughout the car and truck industry each year each year. Its high strength to weight ratio, low cost per unit of strength and 100% recyclability make this material difficult to ignore **[37]**

Fig. 2.5- ADI truck shock absorber brackets.

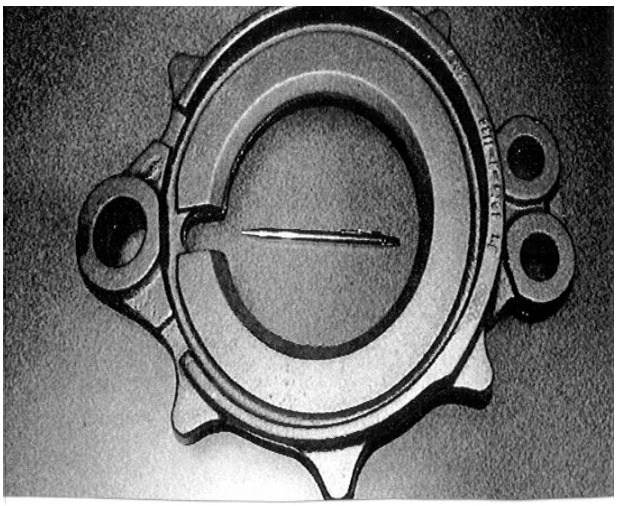

Fig. 2.6- ADI truck brake spider.

Fig. 2.7- ADI truck steering knuckle.

Fig.2.8- ADI truck steering arm

2.6 A Taguchi approach for investigation of wear experiment

Taguchi technique is a technically well-organized mechanism for evaluating and implementing Improvements in products, processes, materials, equipment, and facilities **[38].**

These improvements are pointed at improving the desired features and at the same time reducing the number of faults by studying the key variables monitoring the process and optimizing the procedures or design to yield the best results. This method is valid over a wide range of engineering fields that include processes that manufacture raw materials, sub systems, products for professional and consumer markets. In fact, this technique can be used to any process, be it engineering assembly, computer-aided-design (CAD), banking and service sectors etc.

The aim of the experimental plan is to find the important factors and combination of factors influencing the wear process to attain the minimum wear rate and coefficient of friction. The experiments were established based on an orthogonal array, with the aim of relating the effect of pressure, impact angle and stand of distance (SOD). These design parameters are distinct and inherent feature of the process that influence and determine the composite performance.

The Taguchi method, which is operative to deal with responses, was influenced by multi-variables. It radically reduces the number of experiments that are essential to model the response function compared with the full factorial design of experiments. The major advantage of this technique is to find out his possible interaction plot and main effect between the parameters. This technique is used for process optimization and identification of optimal combination of the factors for a given response. This technique is divided into three main parts, which incorporates all experimentation approaches. The three parts are (1) the planning part (2) the conducting part and (3) the analysis part. Planning phase is the most important phase of the experiment. This technique produces a standard orthogonal array to accommodate the effect of several factors on the target value and defines the plan of experiments. The experimental results are analyzed using analysis of means and variance to study the influence of factors **[39].**

Among the available methods, Taguchi design is one of the most powerful DOE methods for analyzing of experiments. It is widely recognized in many fields particularly in the development of new products and processes in quality control. The salient features of the method are as follows:

- A modest, efficient and systematic method to optimize product/process to improve the performance or reduce the cost.
- Help come to at the best parameters for the optimal conditions with the least number of analytical investigations.
- It is a precisely controlled tool for assessing and executing improvements in products, processes, materials, equipment's and facilities.
- Therefore, the Taguchi method has great potential in the area of low cost experimentation. Thus it becomes an attractive and widely recognized tool to engineers and scientists **[40].**

Taguchi method- based design of experiments involved following steps **[41].**

a. Definition of the problem

A brief statement of the problem under investigation is "comparison of performance of different SG iron with different compositions"

b. Identification of noise factors

The environment in which experiments are performed is the main external source of variation of performance of erosion process. Some examples of the environmental noise factors are temperature, vibrations and human error in operating the process.

c. Selection of response variables

In any process, the response variables need to be selected so that they offer useful evidence about the performance of the process under study.

d. Selection of control parameters and their levels.

e. Identification of control factor interactions

In Taguchi method-based design of experiments, to select a suitable orthogonal array for experimentation, the total degrees of freedom (DOF) needs to be calculated **[42, 43].** The DOF is defined as the number of links between machining parameters that need to be made to determine, which level is better and specifically how much better it is..

f. Selection of the orthogonal array

g. Conducting the matrix experiments (experimental procedure and set-ups)

h. Analysis of the data and prediction of optimum level.

2.7 WEAR

Wear occurs as a natural consequence when two surfaces with a relative motion interact with each other. Wear may be defined as the progressive loss of material from contacting surfaces in relative motion. Scientists have developed various wear theories in which the Physico-Mechanical characteristics of the materials and the physical conditions (e.g. the resistance of the rubbing body and the stress state at the contact area) are taken in to consideration. In 1940 Holm [**44**] starting from the atomic mechanism of wear, calculated the volume of substance worn over unit sliding path.

Wear of metals is probably the most important yet at least understood aspects of tribology. It is certainly the youngest of the tri of topics, friction, lubrication and wear, to attract scientific attention, although its practical significance has been recognizes throughout the ages.

Wear is not an intrinsic material property but characteristics of the engineering system which depend on load, speed, temperature, hardness, presence of foreign material and the environmental condition [**45**]. Widely varied wearing conditions causes wear of materials. It may be due to surface loss or removal of material from one or both of two solid surfaces in a sliding, rolling or impact motion relative to one another. In general cases wear occurs through surface contacts at asperities. During relative motion, material on contacting surface may be removed from a surface, may result in the transfer to the mating surface, or may break loose as a wear particle. The wear resistance of materials is related to its microstructure may take place during the wear process and hence, it seems that in wear research emphasis is placed on microstructure **[46].** Wear of metals depends on many variables, so wear research programs must be planned systematically. Hence researchers have normalized some of the data to make them more useful. The wear map proposed by Lim and Ashby **[45]** is very much useful in this regard to understand the wear mechanism in sliding wear, with or without lubrication.

2.8 TYPES OF WEAR

In most basic wear studies where the problems of wear have been a primary concern, the so-called dry friction has been investigated to avoid the influences of fluid lubricants.

Dry friction' is defined as friction under not intentionally lubricated conditions but it is well known that it is friction under lubrication by atmospheric gases, especially by oxygen **[47].**

A fundamental scheme to classify wear was first outlined by Burwell and Strang **[48].** Later Burwell **[48]** modified the classification to include five distinct types of wear, namely (1) Erosive (2) Abrasive (3) Adhesive (4) Surface fatigue (5) Corrosive.

2.8.1 Erosive wear

Erosive wear can be defined as the process of metal removal due to impingement of solid particles on a surface. Erosion is caused by a gas or a liquid, which may or may not carry, entrained solid particles, impinging on a surface. When the angle of impact is small, the wear produced is closely analogous to abrasion. When the angle of impact is normal to the surface, material is displaced by plastic flow or is dislodged by brittle failure. The schematic representation of the erosive wear mechanism is shown in fig.2.9.

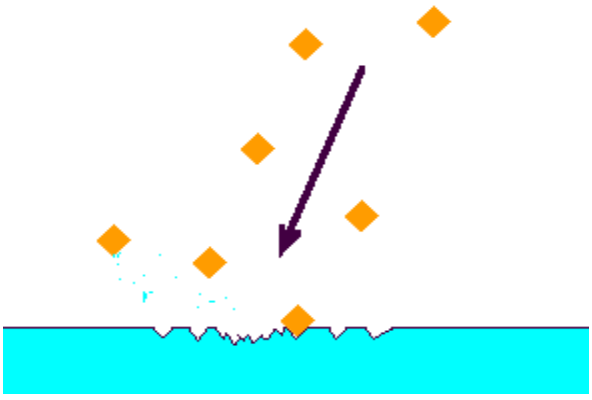

Fig.2.9 Schematic representations of the erosive wear mechanism

2.8.2 Abrasive wear

Abrasive wear can be defined as wear that occurs when a hard surface slides against and cuts groove from a softer surface. It can be account for most failures in practice. Hard particles or asperities that cut or groove one of the rubbing surfaces produce abrasive wear. This hard material may be originated from one of the two rubbing surfaces. In sliding mechanisms, abrasion can arise from the existing asperities on one surface (if it is harder than the other), from the generation of wear fragments which are repeatedly deformed and hence get work hardened for oxidized until they became harder than either or both of the sliding surfaces, or from the adventitious entry of hard particles, such as dirt from outside the system.

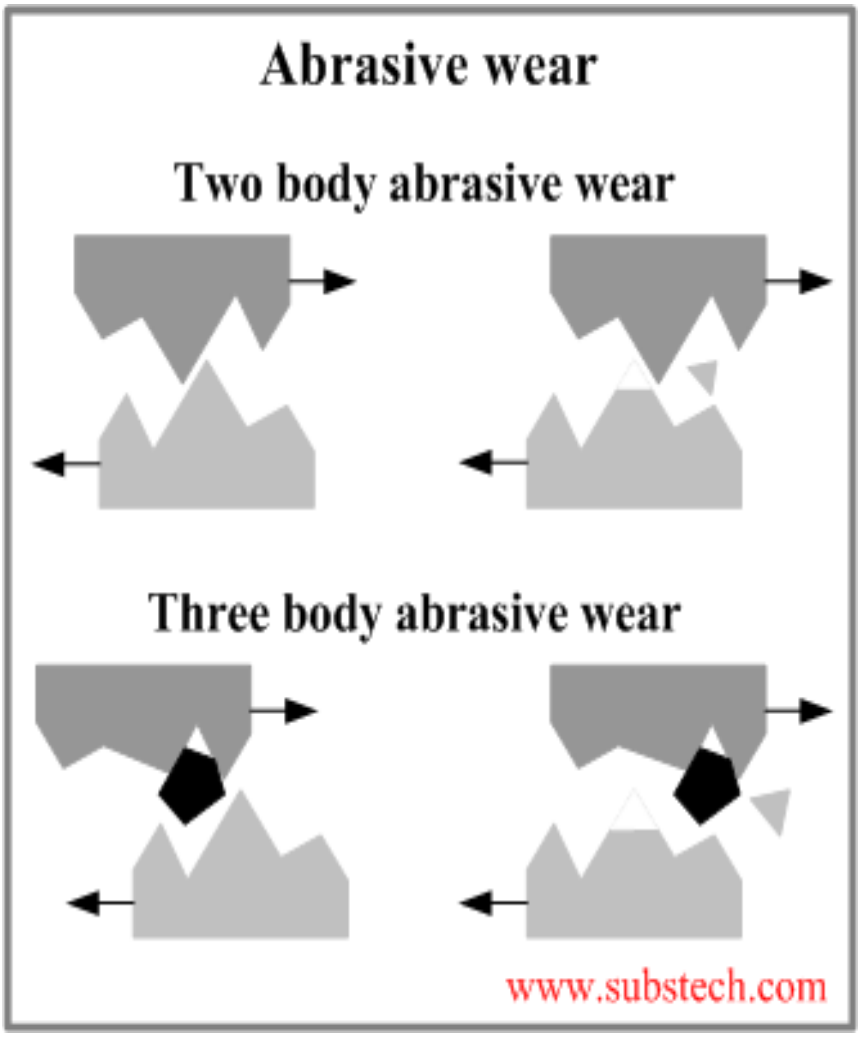

Fig. 2.10 Schematic representations of the abrasion wear mechanism.

Two body and three body abrasive wear as shown in fig. 2.10 occurs when one surface (usually harder than the second) cuts material away from the second, although this mechanism

very frequently changes to three body abrasion as the wear debris then acts as an abrasive between the two surfaces. Abrasives can act as in crushing where the abrasive is fixed relative to one surface or as in lap up where the abrasive tumbles producing a series of indentations as opposite to a scratch. According to the recent tribological survey, abrasive wear is responsible for the largest amount of material loss in industrial practice **[49].**

2.8.3 Adhesive wear

Adhesive wear can be defined as wear due to chemical bonding between contacting solid surfaces leading to material transfer between the two surfaces or the loss from either surface. For adhesive wear as shown in fig. 2.11 to occur it is necessary for the surfaces to be in close contact with each other. Surfaces, which are held apart by lubricating films, oxide films etc. reduce the tendency for adhesion to occur.

Fig. 2.11 Schematic representations of the adhesive wear mechanism.

2.8.4 Surface fatigue wear

Wear of a solid surface caused by fracture arising from material fatigue. The term 'fatigue' is mostly used to the failure phenomenon where a solid is subjected to cyclic loading involving tension and compression above a certain critical stress. Cyclic loading causes the generation of micro cracks, usually below the surface, at the site of a pre-existing point of weakness. On subsequent loading and unloading, the micro crack propagates. Once the crack reaches the critical size, it changes its direction to emerge at the surface, and thus flat sheet like particles is detached during wearing process. The number of stress cycles required to cause such failure decreases as the corresponding magnitude of stress increases. Vibration is a common cause of fatigue wear.

2.8.5 Corrosive wear

Most metals are thermodynamically unstable in air and react with oxygen to form an oxide, which commonly develop layer or scales on the surface of metal or alloys when their interfacial bonds are poor. Corrosion wear is the gradual eating away or deterioration of unprotected metal surfaces by the effects of the atmosphere, acids, gases, alkalis, etc. This type of wear creates pits and perforations and may eventually dissolve metal parts.

2.9 SYMPTOMS OF WEAR

Literature available on the rate controlling wear mechanism demonstrated that it may change abruptly from one another at certain sliding velocities and contact loads, resulting in abrupt increases in wear rates. The conflicting results in the wear literature arise partly because of the differences in testing conditions, but they also make clear that a deeper understanding of the wear mechanism is required if an improvement in the wear resistances of the coating is to be achieved. This in turn requires a systematic study of the wear under different stresses, velocities and temperatures. It is generally recognized that wear is a characteristic of a system and influenced by many parameters. Laboratory scale investigation if designed properly allows careful control of the tribo system where by the effects of different variables on wear behavior of the coating can be isolated and determined. The data generated through such investigation under controlled conditions may help in correct interpretation of the results.

Types of wear	Symptoms	Appearance of the worn-out surface
Erosion	Presence of abrasives in the fast moving fluid and short abrasion furrows	Waves and troughs.
Abrasive	Presence of clean furrows cut out by abrasive particles	Grooves
Adhesive	Metal transfer is the prime symptoms	Seizure, catering rough and torn-out surfaces.
Corrosion	Presence of metal corrosion products.	Rough pits or depressions.
Fatigue	Presence of surface or subsurface cracks accompanied by pits and spalls	Sharp and angular edges around pits.
Impacts	Surface fatigue, small sub - micron particles or formation of spalls	Fragmentation, peeling and pitting
Delamination	Presence of subsurface cracks parallel to the surface with semi-dislodged or loose flakes	Loose, long and thin sheet like particles
Fretting	Production of voluminous amount of loose debris	Roughening, seizure and development of oxide ridges
Electric attack	Presence of micro craters or a track with evidence of smooth molten metal	Smooth holes

Table 2.1 Symptoms and appearance of different types of wear **[50].**

A summary of the appearance and symptoms of different wear mechanism is indicated in Table 2.2 and the same is a systematic approach to diagnose the wear mechanisms.

A typical model, demonstrating the rate of erosion dependent on size and velocity of particle on impacting the substrate is shown in fig.2.12. The increase in impact velocity or particle diameter clearly accelerates erosion damage. From the statistic that an increase in particle velocity or size leads to larger or deeper indentations as schematically shown in Fig. 2.7, deviations in k2 and k3 values from the hypothetical ones (k2 =2, k3 = 0) indicate the true effects of impact velocity and particle diameter which are associated with the relative aggressiveness of indentation. The larger or deeper is the indentation the greater amount of material is removed from the rim of the indentation

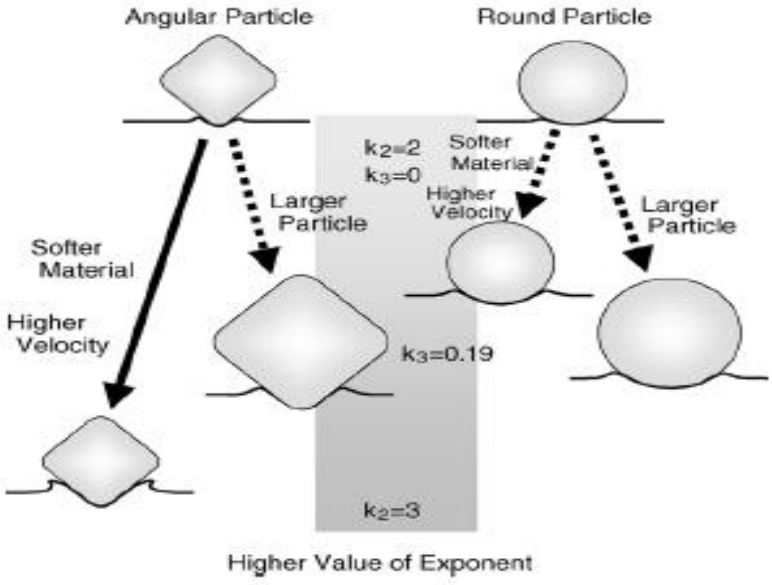

Fig. 2.12 Model of the effects of impact parameters on exponents k_2 and k_3.

2.10 RECENT TRENDS IN METAL WEAR RESEARCH

Much of the wear researches carried out in the 1940's and 1950's were conducted by mechanical engineers and metallurgists to produce data for the creation of motor drive, trains, brakes, bearings, bushings and other types of moving mechanical assemblies **[51].**

It developed apparent during the survey that wear of metals was a prominent subject in a large number of the responses about some future priorities for research in tribology. Some 22 experienced technologists in this field, who attended the 1983 'Wear of Materials Conference' in Reston, prepared a ranking list **[52].** Their suggestions with top priority were further research of the mechanism of wear and this no doubt reflects the judgments that particular effects of wear should be studied against a background of the basic physical and chemical processes involved in surface relations. The list proposed is shown in table 2.2.

Peterson **[53]** reviewed the development and use of tribo-materials and established that metals and their alloys are the most common engineering materials used in wear applications. Grey cast iron for example has been used as early as 1388. Much of the wear research directed over the past 50 years is in ceramics, polymers, composite materials and coatings **[54].**

Wear of metals encountered in industrial conditions can be grouped into classes shown in table 2.3. Though there are situations where one type changes to additional or where two or more mechanism plays together.

Ranking	Topics
1.	Mechanism of Wear
2.	Surface Coatings and treatments
3.	Abrasive Wear
4.	Materials
5.	Ceramic Wear
6.	Metallic Wear
7.	Polymer Wear
8.	Wear with Lubrication
9.	Piston ring-cylinder liner Wear
10.	Corrosive Wear
11.	Wear in other Internal Combustion Machine Components

Table 2.2 Priority in wears research **[55].**

Types of wear in industry	Approximate percentage involved
Abrasive	50
Adhesive	15
Erosion	8
Fretting	8
Chemical	5

Table 2.3 Type of wear in industry **[54].**

2.11 ANN METHOD

An ANN is a computational system that pretends the microstructure (neurons) of biological nervous system. The most basic components of ANN are modeled after the structure of brain. Motivated by these biological neurons, ANN is composed of simple elements working in parallel. It is the simple gathering of the basic artificial neurons. This gathering occurs by creating layers, which are then related to one another. The multilayered neural network has been utilized in the most of the research works for material science. A software package NEURALNET for neural computing developed by Rao and Rao [56] using back propagation algorithm is used as the forecast of erosion wear rate at different impact angles, stand of distance and pressure.

2.12 EROSIVE WEAR CHARATERISTICS OF SPHEROIDAL CARBIDES CAST IRON

The leading factors that influence erosion are mainly related with the mechanical properties of objective materials, especially, the hardness of the materials. In addition to the hardness, the shapes, hardness and sizes of impact particles, impact speed, and impact angle of particles also affect the amounts of materials removed and erosion characteristics of materials **[57–60].**

Look over earlier works of other researchers, many erosive wear testing were proposed to explain the mechanism of objective materials. From the research on the effect of impact angle, it is generally concluded that erosive wear of material depends on the impact angle of particles and a material has weak angle and strong angle to particles impacting.

The erosion of ductile material stroke by angular abrasive particles was formulated by Finnie **[61]** at 1960. On the basis of two dimensions cutting theory, Finnie established expressions of erosive wear amount to approximately explain the influence of impact angle and impact speed of abrasive on erosion. But the predicted value underestimates erosion at high-impact angles disagree the experimental value of erosion at 90◦. Bitter **[62, 63]** developed the Finnie's theory with very complete study of the problem, and documented that it is necessary to exceed threshold conditions in order to cause damage. The dependence on impact angle was explained by the theory of what was termed "cutting" erosion occurring at glancing impact whilst "deformation" erosion predominated at angles close to the normal. Neilson and Gilchrist **[64]** subsequently simplified Bitter's analysis, and then Tilly **[65–68]** had introduced the incubation effect in the influence of impact angle and presented a two-stage mechanism on ductile erosion. Hutchings and winter **[57, 58]** introduced the ploughing method to explain the erosive wear mechanism. As is known to all, these studies laid the foundation of erosion mechanism. However, it is found that impact angle dependency of erosive wear differs from one to another not only because of characteristic of target materials but also because of property of impact particles and impact condition. Accordingly, it seems unreasonable that direct application of the results of previous work in the erosive wear assessment of other industrial materials. And then recently, many of researchers **[11–14]** mainly aimed at the erosive wear of composite material, superalloy, hard surface coatings, high chromium white cast iron, and so on; among these, high chromium white cast irons have been defined previously to good wear-resistance materials in abrasive condition, however, the presence of dendrite or flaky shaped carbides embedded in matrix drew them occur stress concentration easily to limit their wear resistance. Therefore, we developed the cast irons with spheroidal carbides embedded in matrix, and there has little attention on the study of these kinds of cast irons. The cast irons with spheroidal carbides embedded in matrix, and there has little attention on the study of these kinds of cast irons.

CHAPTER 3

EXPERIMENTAL SET UP & METHODOLOGY

- Introduction
- Melting & Casting
- Optical Microscopy
- Air jet erosion test rig machine
- Vickers hardness test
- Introduction about XRD machine

3.0 INTRODUCTION

This section deals with the details of the experimental procedures used in this study. This study include test specimen preparation, After sample preparation, the materials have been subjected to a series of tests, e.g., microstructural investigation of the surfaces and cross sections, Vickers hardness measurement, X - ray diffraction studies, air jet erosion wear test etc. The details of each process are described in this section.

3.1 MATERIALS AND IT'S PREPARATION

The materials were melted in a 250 kg induction furnace with medium frequency. Charges consisting 50kg pig iron (C=4.17%, Si=1.66%, Mn=0.138%, S=0.024%, P=0.060%), 100kg S.G return (C=3.62%, Si=2.12%, Mn=.19%, S=0.010%, P=0.026%) and 150kg steel scrap (C=0.038%, Si=0.037%, Mn=0.135%, S=0.005%, P=0.015%) were melted in furnace. At this time the sample was taken from the melt for final chemical analysis. The pouring temperature was 1380˚C. Similarly other five melts were prepared with varying chemical composition and all melts were properly post inoculated. The chemical compositions of all the raw materials used are obtained from manufacturer's analysis.

The chemical compositions of the six cast iron specimens used in this study are given in Table 1. The all six irons with different graphite morphologies and chemical compositions were used for investigation. And these specimens also differentiate with their carbon equivalent. Carbon equivalent is calculated by formula.

[% C.E. = %C + 0.3% Si + 0.33 % S - 0.027% Mn +0.4 % P]

samples	type	grade	C %	Si%	Mn%	S%	P%	Cr%	Ni%	Mg%	Cu%	C.E.
ER1	SG	CI	3.42	2.26	0.13	0.008	0.026	0.03	0.24	0.042	0.05	4.10353
ER2	SG	CI	3.48	2.32	0.19	0.008	0.031	0.04	0.48	0.039	0.01	4.1859
ER3	SG	CI	3.54	2.13	0.16	0.01	0.034	0.04	0.18	0.051	0.051	4.19077
ER4	SG	CI	3.5	2.24	0.19	0.011	0.036	0.03	0.39	0.062	0.013	4.19516
ER5	SG	CI	3.66	2.06	0.17	0.01	0.023	0.04	0.38	0.035	0.01	4.28591
ER6	SG	CI	3.72	2.01	0.17	0.01	0.029	0.03	0.11	0.044	0.37	4.33

Table -3.1 Different composition of SG iron samples (CI-cast iron, SG-spheroidal gray cast iron

In order to obtain optimum mechanical properties several impact tests were carried out on each material at each austempering holding time. The specimens with optimum impact energy were used for wear tests.

3.3 AIR JET EROSION TEST RIG MACHINE

An air jet erosion test rig (ASTM G76) used to test the erosion of specimens in this research. The schematic view of the testing machine is showed in Fig.-1

Fig.-3.1 Details of erosion test rig. (1) Sand hopper, (2) Conveyor belt system for Sand flow, (3) Pressure transducer, (4) Particle-air mixing chamber, (5) Nozzle, (6) X–Y and h axes assembly, (7) Sample holder.

The air jet erosion tester will evaluate the erosion resistance of variety of materials including ceramics, metals, polymers, coatings and composites conforming to ASTM G 76 specifications.

Sl. No.	Description	Required Parameters
1.	Sample Temperature range.	RT – 400 deg C
2.	Angle of inclination of sample during Testing w.r.t. the jet of erodent particles.	5 to 90 deg
3.	Air pressure	Upto 6 bar
4.	Air velocity	Upto 100 m/s
5.	Air flow rate	Upto 100 lpm
6.	Particle velocity	Upto 30 m/s
7.	Particle feed rate	2 to 10 g/min
8.	Specimen size	To be mentioned – Approx. 75mmx25mmx6mm preferable
9.	X, Y and Z adjustment and tilting	To be provided
10.	Collection of Erodent after testing in removable enclosure	To be provided
11.	Sound and dust proof enclosure	To be provided
12.	Nozzles	3 mm and 5 mm diameter to be provided
13.	Additional features	Air drier and Air filter must be embedded in the system

Table 3.2 Technical Specification for Air Jet Erosion Tester

An Air jet erosion test rig was used to test erosive wear of target materials in the present investigation. Angular (irregularly shaped) silica sand was used as impact particles. The specimens were mounted into the test stage directly below the nozzle with using different stand of distance (distance between tip of the nozzle to surface of the specimen) and also Samples were

eroded with silica sand at different impingement angles (i.e. 30˚, 45˚, and 60˚). The room temperature erosion test facility used in the present investigation. The setup is capable of creating a uniform erosive situation for evaluating erosion wear resistance of the prepared SG iron samples. Dry silica sand is used as the erodent. The particles fed at a constant rate are made to flow with compressed air jet compressor to impact the specimen, which can be held at various angles with respect to the flow direction of erodent using a swivel and an adjustable sample clip. The samples were cleaned in acetone, dried and weighed to an accuracy of ±0.1mg accuracy using a precision electronic balance. The surface of material eroded in the test rig for 10 min and weighed again to determine the weight loss. The procedure is repeated for all samples. The rig consists of an air compressor, a particle feeder, and an air particle mixing and accelerating chamber. The compressed dry air is mixed with the erodent particles, which are fed at a constant rate from a conveyor belt-type feeder in to the mixing chamber and then accelerated by passing the mixture through a tungsten carbide converging nozzle of 5 mm diameter. These accelerated particles impact the sample, and the sample could be held at various angles with respect to the impacting particles using an adjustable sample holder.

3.3 OPTICAL MICROSCOPY

Materials used in this research were characterized by OLYMPUS BX51M optical microscope. The specimens measuring 10mm×15mm were used for metallographic processing. In this analysis we take the images of different eroded surfaces.

3.4 X-RAY DIFFRACTION STUDIES

The X-Ray diffraction (XRD) analysis was performed for all six samples. XRD was performed 30 KV and 20 mA using a Cu- Kα target diffractmeter. Scanning was done in angular range 2θ from 40° to 90° at a scanning speed of 2°/min. The profiles were analyzed on computer by using X‟ Pert High Score Software to obtain the peak position and integrated intensities of the austenite and ferrite.

Fig 3.2 -XRD machine

3.5 VICKERS HARDNESS TESTER

The heat treated samples were polished in emery papers of different grits for hardness measurement. Vickers Hardness test was carried out at room temperature to measure the hardness of the SG iron samples. The load was applied through the diamond indenter for 10 seconds during testing of all the treated and untreated samples.

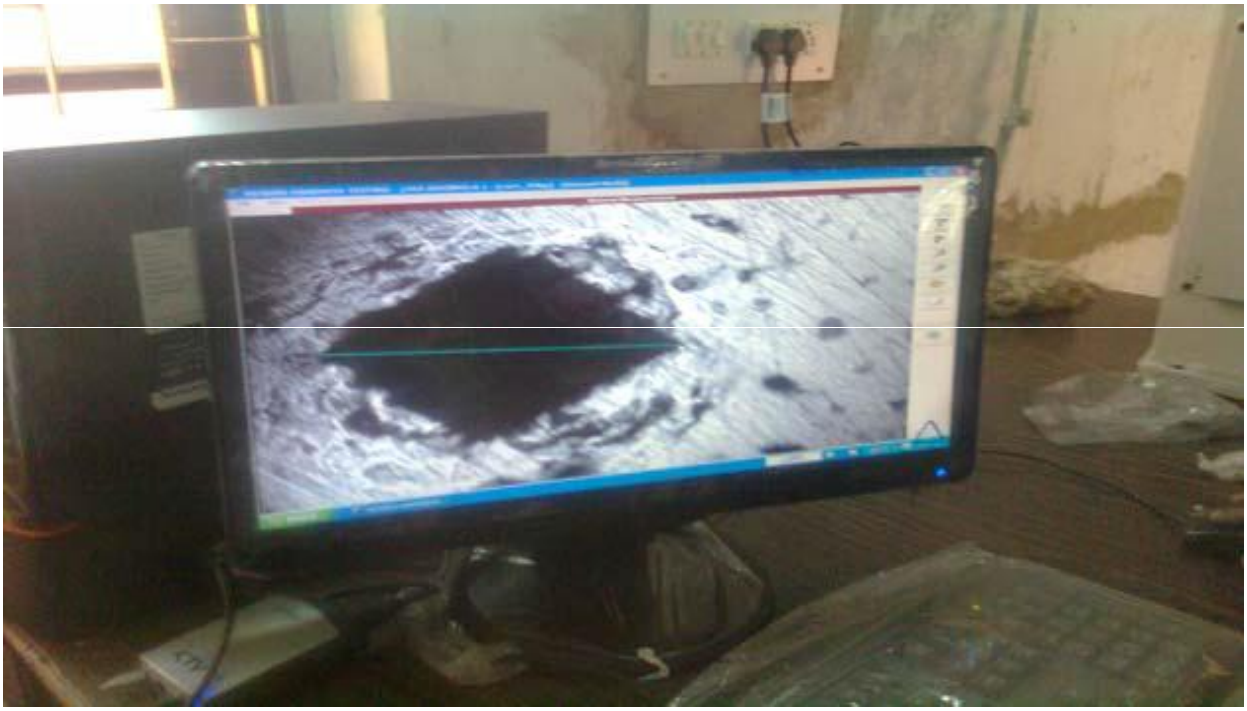

Fig. 3.3. showing hardness measurement

The shape of the indentation is shown in the figure. Three measurements for each sample were taken from one point to another through the central line of the casting specimen and averaged to get final hardness results. A load of 20 kg was applied to the specimen for 10 seconds. Then the depth of indentation was noted by a programme installed in the computer of arbitrary hardness numbers. Then these values were changed to in terms of required hardness numbers (as Brinelle‟s or Vickers hardness numbers).

CHAPTER 4

RESULT AND DISCUSSION

- Introduction
- Vickers hardness measurements
- XRD phase composition analysis
- Solid particle erosion wear behavior
- Taguchi experimental design result
- Microstructural Investigation

4.1 INTRODUCTION

This chapter introduces the result of experiment utilized to characterize the SG iron. The results of various experiments are presented and discussed in this chapter. Characterization of the SG irons with different composition was done with respect to their excellence and tribological performance. The obtained data has been correlated with standard results. The results are discussed hereunder.

4.2 VICKERS HARDNESS MEASUREMENTS

In the erosion test, it is recognized that the work-hardening effect which resulted from impact of solid particles on material surface was happened. The harnesses of specimens before and after erosion test were measured through Vickers hardness test.

Result show that the differences of hardness before and after test, we can see that there were happened the work-hardening effects on the material surface. The results of Vickers hardness were dramatically increased after erosion test for all samples. The surface hardness of samples before erosion test is 183.5HV20, 199HV20, 125.5HV20, 228HV20, 206.5HV20 and 214HV20 but after erosion test hardness are increases 225.5HV20, 250.5HV20, 175.8HV20, 286.5HV20, and 295HV20 respectively. From this fact, we can understand that it is true that erosion rate depends heavily on hardness of surface of material [62]; however, initial hardness of samples increases due to work hardening.

4.3 XRD PHASE COMPOSITION ANALYSIS

XRD plots between intensity and 2θ diffraction angle for different samples are shown in the graphs below. XRD was performed 30 KV and 20 mA using a Cu- Kα target diffractmeter. Scanning was done in angular range 2θ from 40° to 90° at a scanning speed of 2°/min. The profiles were analyzed on computer by using X‟ Pert High Score Software to obtain the peak position and integrated intensities of the austenite and ferrite. The {111}, {200}, and {211} planes of ferrite were used to estimate the lattice parameter.

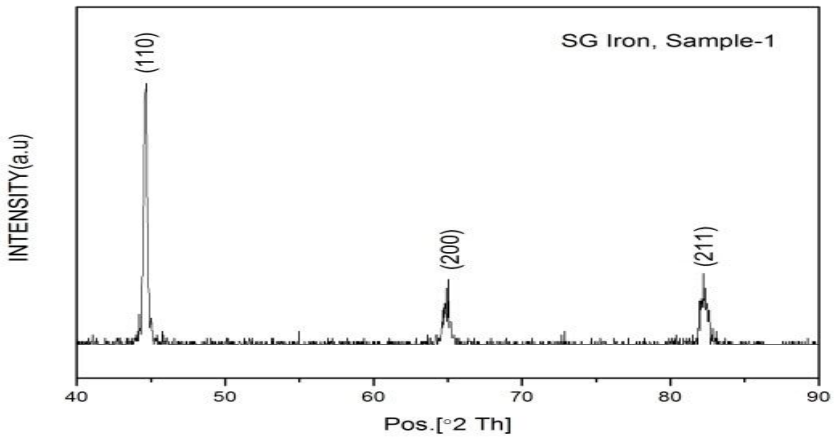
SG Iron, Sample-1
(110)
(200)
(211)
INTENSITY(a.u)
40
50
60
70
80
90
Pos.[°2 Th]

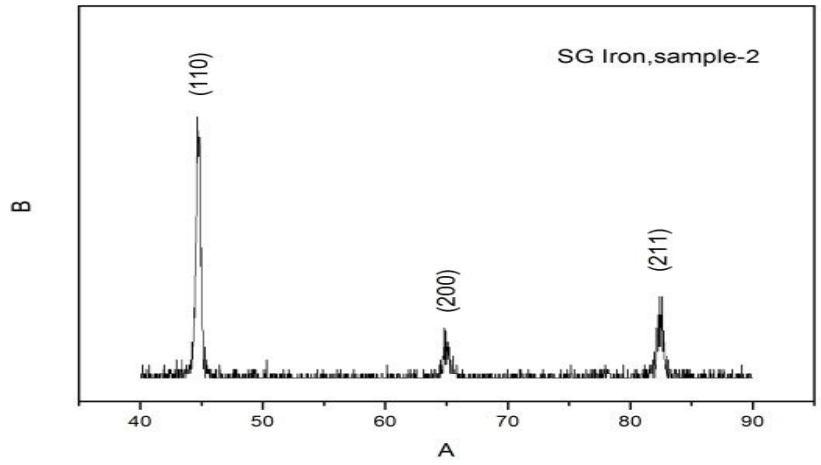
SG Iron,sample-2
(110)
(200)
(211)
B
40
50
60
70
80
90
A

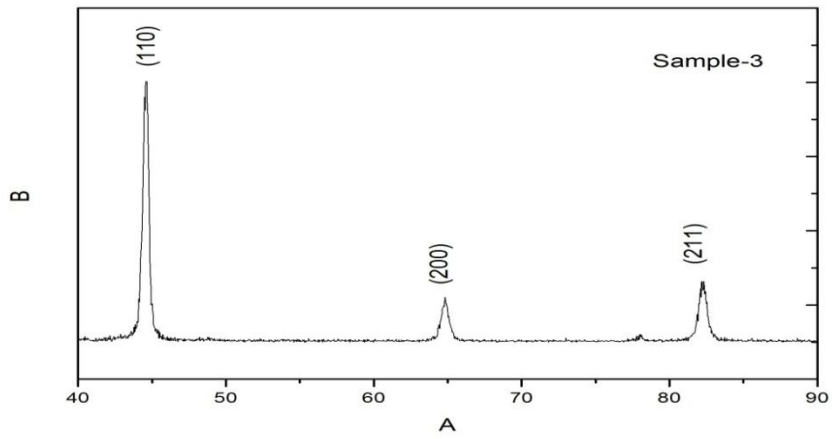
Sample-3
(110)
(200)
(211)
B
40
50
60
70
80
90
A

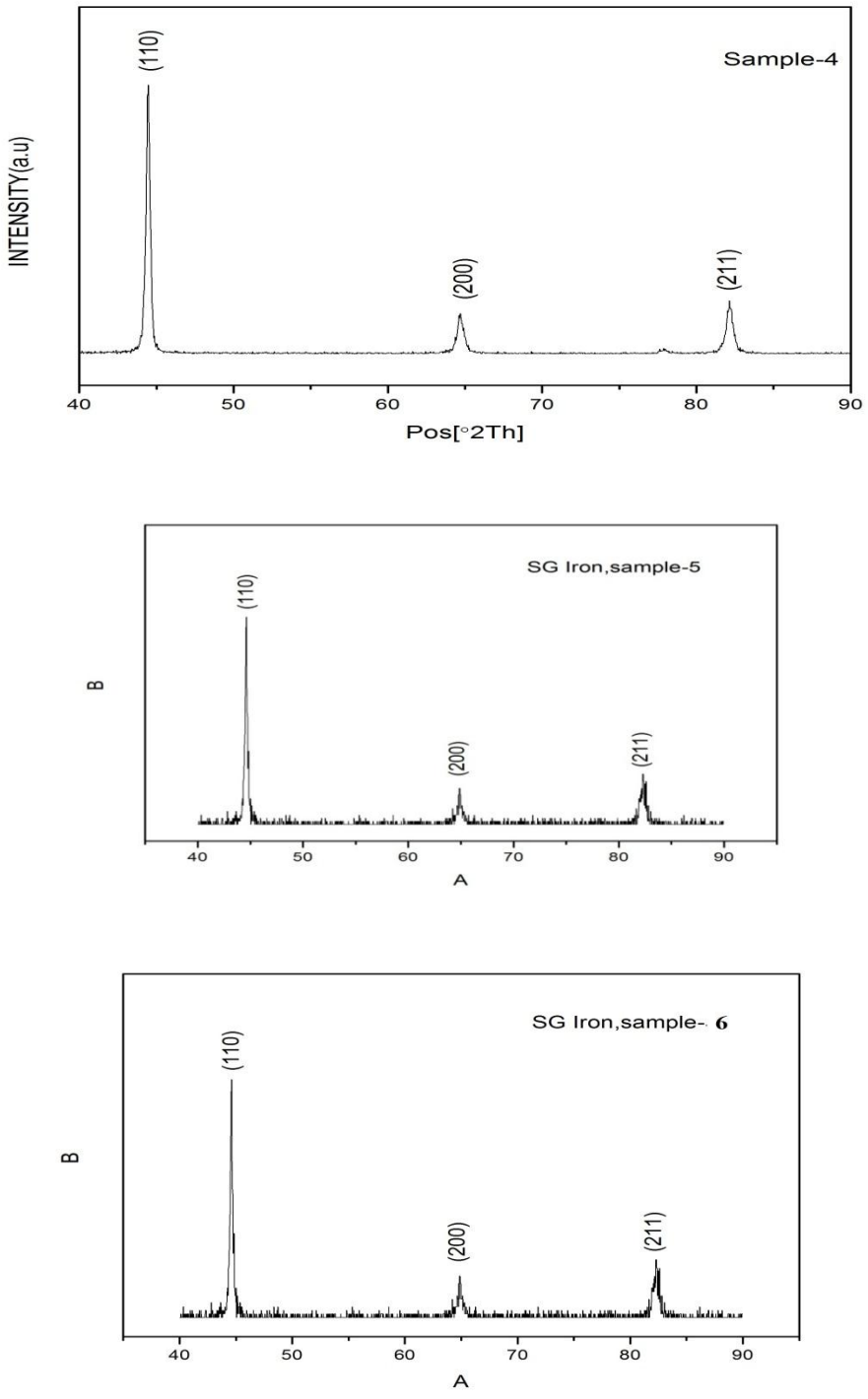

A- POSITION (˚2Th), B-INTENSITY (a.u.)

Fig 4.1: Diffraction patterns of different SG iron samples (sample 1 to 6)

The angular range that was examined includes peaks for and ferrite (α). The integrated intensities of each peak were used to calculate the relative amounts of the phases present.

However, no prominent asymmetry is visible on the low angle side of the ferrite peak, which suggests an absence of any measurable amount of martensite.

An estimate of the ferritic cell size (*d*) was obtained from the X-ray diffraction profile from the breadth of the {211} diffractometer peaks of ferrite using the Scherer formula:

$$d=0.9\lambda / \beta \cos\theta$$

$$d=2\varepsilon \tan\theta$$

Where, λ is the wavelength, β is the breadth of the (211) peak of ferrite at half height in radians, θ is the Bragg angle and 2ε is effective lattice microstrain.

From above calculation crystallite-size for ferrite phase varies from 17nm to 40nm and microstrain varies from 0.0022 to 0.0039.

In this study we deal with determination of crystallite-size distribution and microstrain measurement of SG iron by the means of x-ray diffraction line broadening. The deformation process imposed on materials yield the formation of microstrain and crystallite size domains with in each grain which are somehow related to mechanical behavior of material [69].

4.4 SOLID PARTICLE EROSION WEAR BEHAVIOUR

Numerous erosion models/correlations were developed by many researchers to offer a quick answer to design engineers in the absence of a comprehensive practical approach for erosion prediction. The erosion model suggested by Bitter [62,63] assumed that the erosion occurred in two mechanisms; the first was caused by repeated deformation during impacts that eventually results in the breaking loose of a piece of material while the second was caused by the cutting action of the moving particles. Comparisons between the obtained data and the test results showed a good agreement. It was determined that cutting wear prevails in places where the impact angles are small (such as in risers and straight pipes) and it is sufficient to use hard material in such places to reduce erosion. Glaeser and Dow [70] proposed another two-stage mechanism for explaining different aspects of the erosion process for ductile materials. In the

first stage, the particles indent the target surface, causing chips to be removed and some material to be extruded to form susceptible hillocks around the scar. The second stage was the one in which the particles break up on impact causing fragments to be projected radially to produce a secondary damage. A correlation was presented relating erosion to the energy required to remove a unit mass and the particle velocity and size. The calculated values of erosion rate were compared with the experimental data and a practical agreement was found, however, the validity of the work was limited to ductile materials and could not be generalized to include other materials. Other erosion models were suggested by Laitone [71], Salama and Venkatesh [72], Bourgoyne [73], Chase et al. [74], McLaury [75], Svedeman and Arnold [76], and Jordan [77]. Recently, Shirazi and McLaury [78] presented a model for predicting multiphase erosion in elbows. The model was developed based on general empirical information gathered from many sources, and it accounts for the physical variables affecting erosion, including fluid properties, sand production rate and size, and the fluid-stream composition. An important different feature of this model was the use of the characteristic impact velocity of the particles.

In most erosion processes, target material removal typically happens as the result of a large number of impacts of irregular angular particles, usually carried in pressurized fluid streams. The fundamental mechanisms of material removal, however, are more easily understood by analysis of the impact of single particles of a known geometry. Such fundamental studies can then be used to guide development of erosion theories involving particle streams, in which a surface is impacted repeatedly. Single particle impact studies can also reveal the rebound kinematics of particles, which are very significant for models which take into account the change in erosive potential due to collisions between incident and rebounding particles, [79, 80].

In present investigation erosion rate depends on many factors size of impact particle, impact angle, stand of distance (it is distance between nozzle tip to surface of material), pressure, velocity of particle, inner diameter of nozzle etc. but we considering the only main three factors impact angle, pressure and stand of distance.

4.5 TAGUCHI EXPERIMENTAL DESIGN RESULT

The aim of the experimental plan is to find the important factors and combination of factors influencing the wear process to achieve the minimum wear rate and coefficient of friction. The experiments were developed based on an orthogonal array, with the aim of relating the influence of impact angle, pressure, stand of distance. These design parameters are distinct and intrinsic feature of the process that influence and determine the material performance.

The erosion curves are plotted from the results of erosion tests conducted for different parameter (impact angle, pressure and stand of distance) keeping all other parameters constant (impact velocity in m/sec and erodent size in mm). It is interesting to note that the Taguchi experimental design method identified the pressure and impact angle are the most influencing factors that affect erosion rate for all samples of SG irons and standoff distance is less effect on erosion wear rate. In this analysis main effect plot obtained for different samples which are shown in the fig.4.2, fig. 4.4, fig. 4.6, fig. 4.8, fig 4.10 and fig. 4.12.

From the interaction plot it is observed that there is no more interaction between any of factors with each other as there is no crossing between lines as shown in the fig.4.3, fig. 4.5, fig. 4.7, fig. 4.9, fig 4.11 and fig. 4.13.

From the fig.4.2, erosion rate decreases with increase in stand of distance. At 40 mm stand of distance, erosion rate is more as compare to 60 mm stand of distance. Also at higher pressures, erosion rate is high as compare to that of lower pressures. It is frequently observed that the angle of maximum erosion rate is close to 30 to 40 degree in ductile erosion of metal [81, 82, and 83].

In present investigation response table 4.1 obtained by the Taguchi analysis which show that pressure is highly influencing variable for erosion rate as compare to impact angle and stand of distance was found to be less influencing for all different compositions of SG iron.

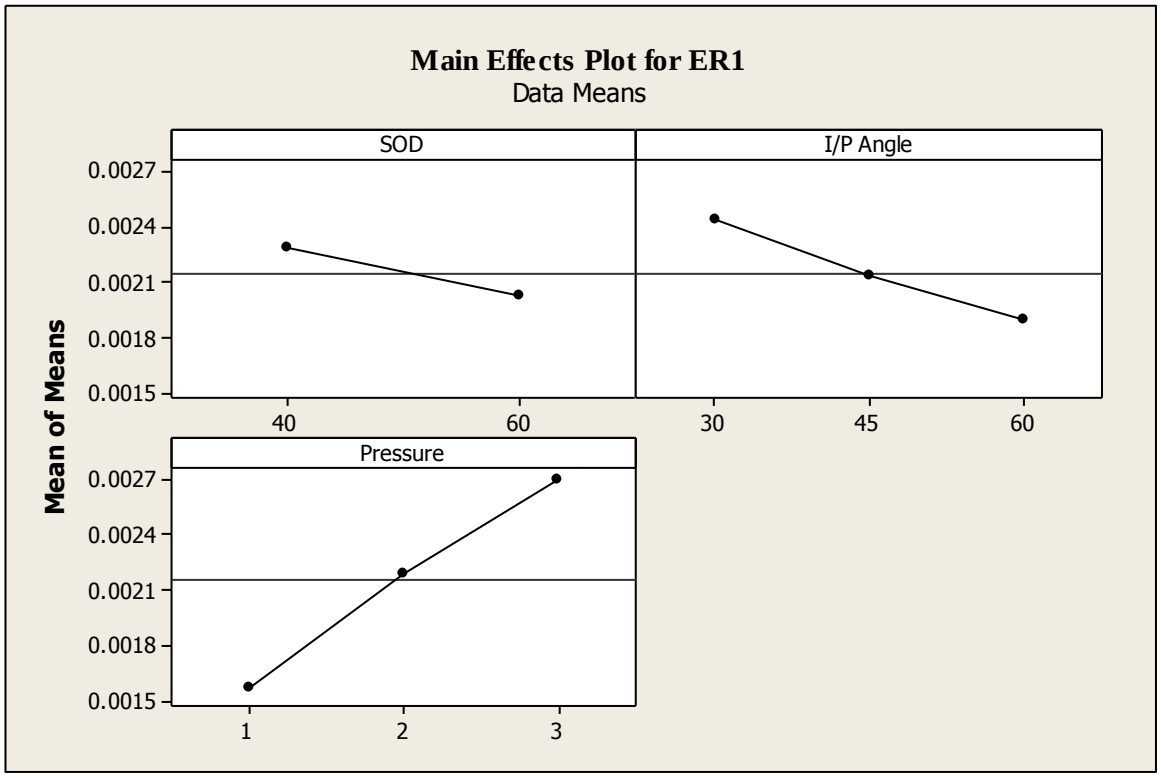

Fig. 4.2- Effect of control factors on erosion rate. (For sample 1)

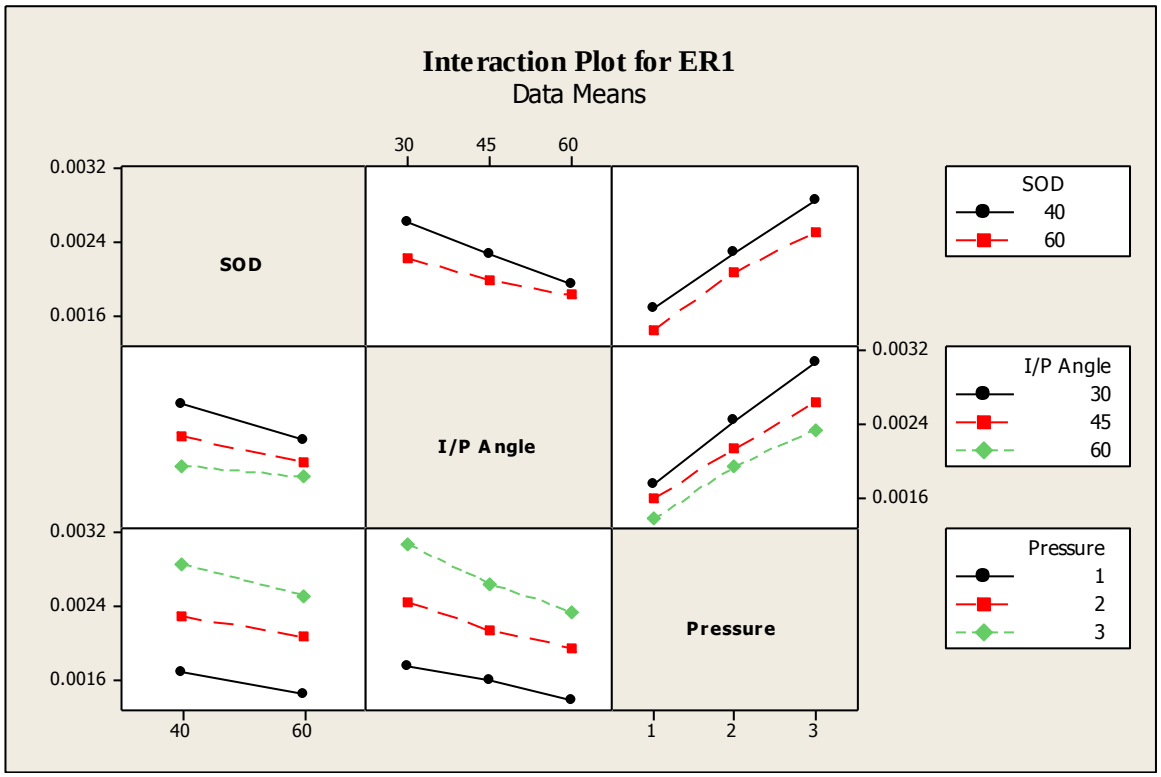

Fig. 4.3- Interaction plot (For sample 1)

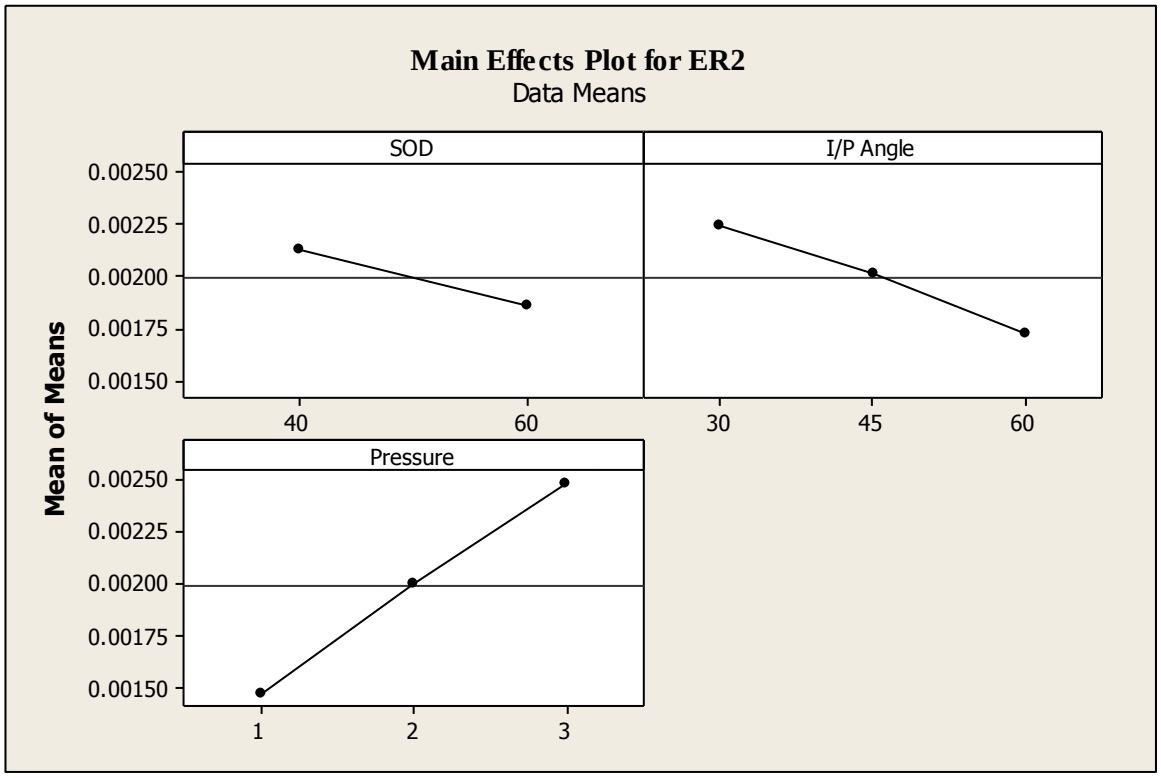

Fig.4.4- Effect of control factors on erosion rate. (For sample 2)

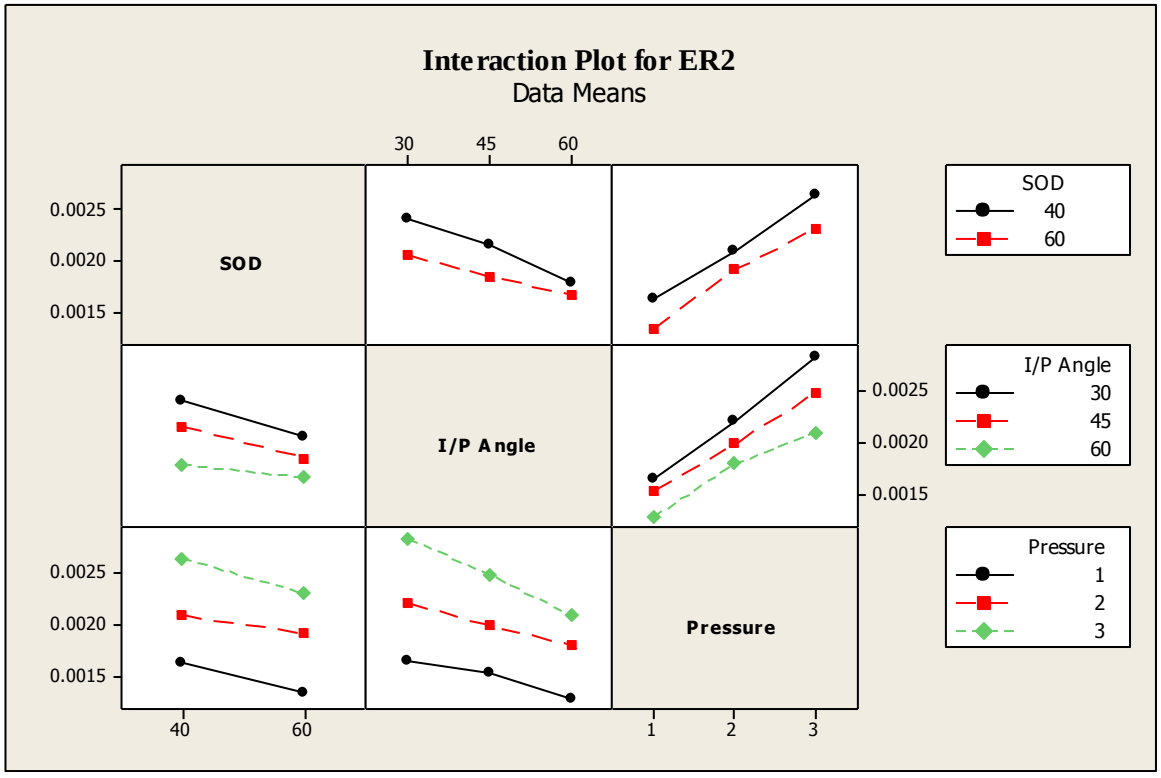

Fig. 4.5 - Interaction plot (For sample 2)

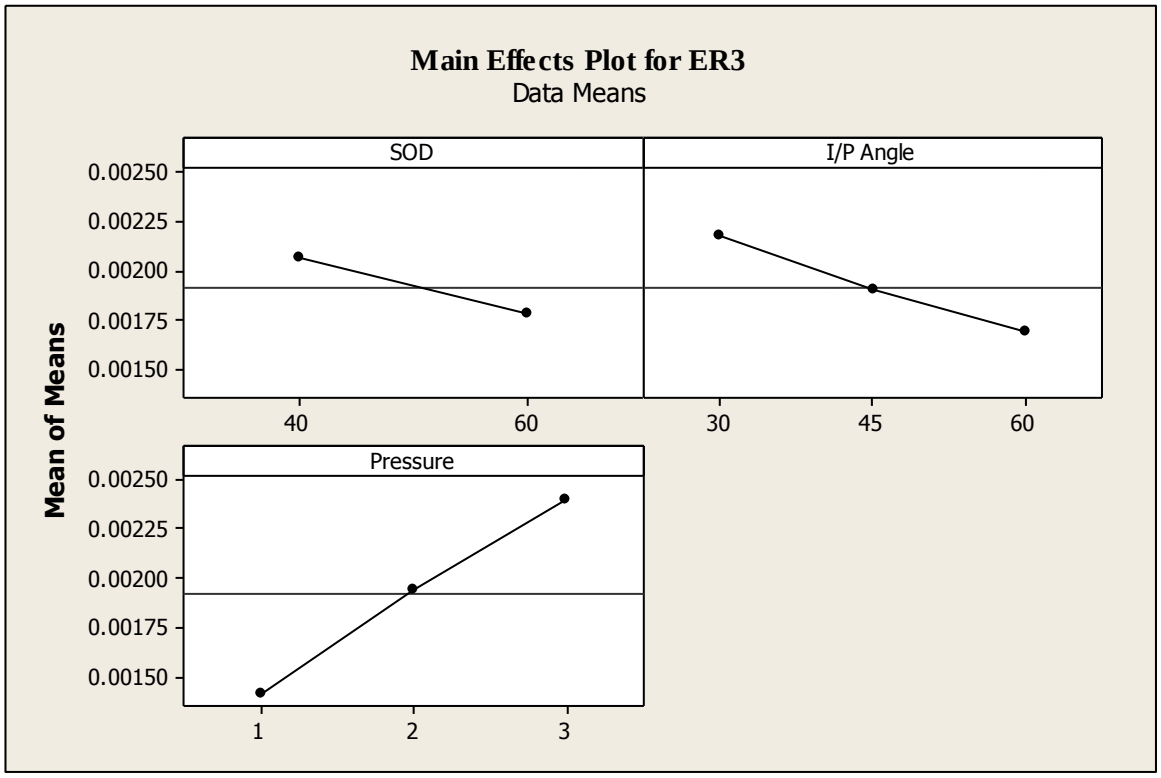

Fig.4.6 - Effect of control factors on erosion rate. (For sample 3)

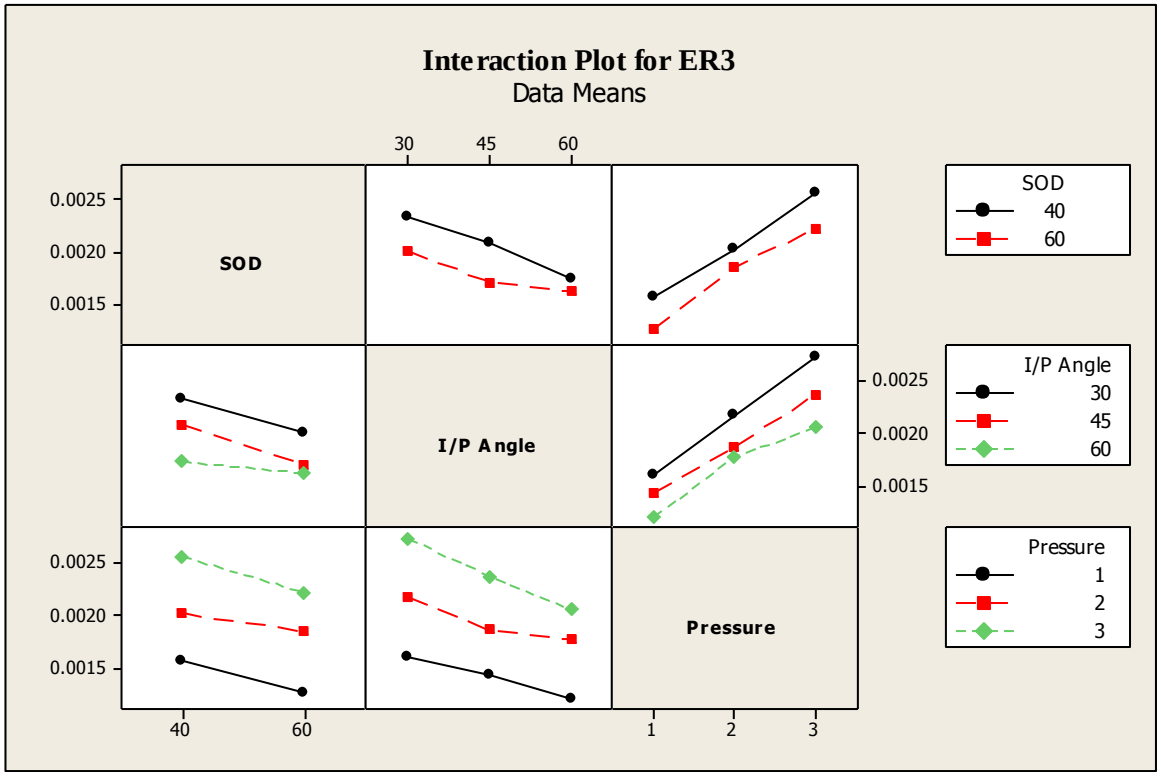

Fig. 4.7- Interaction plot (For sample 3)

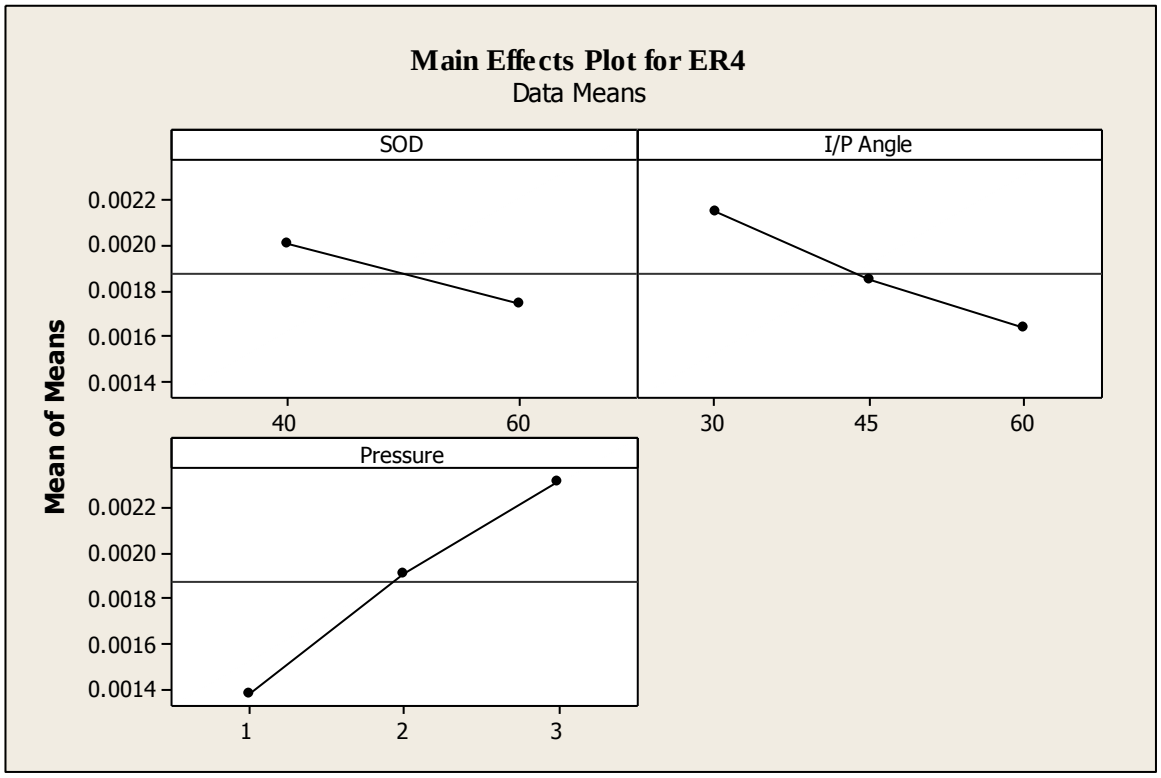

Fig. 4.8- Effect of control factors on erosion rate. (For sample 4)

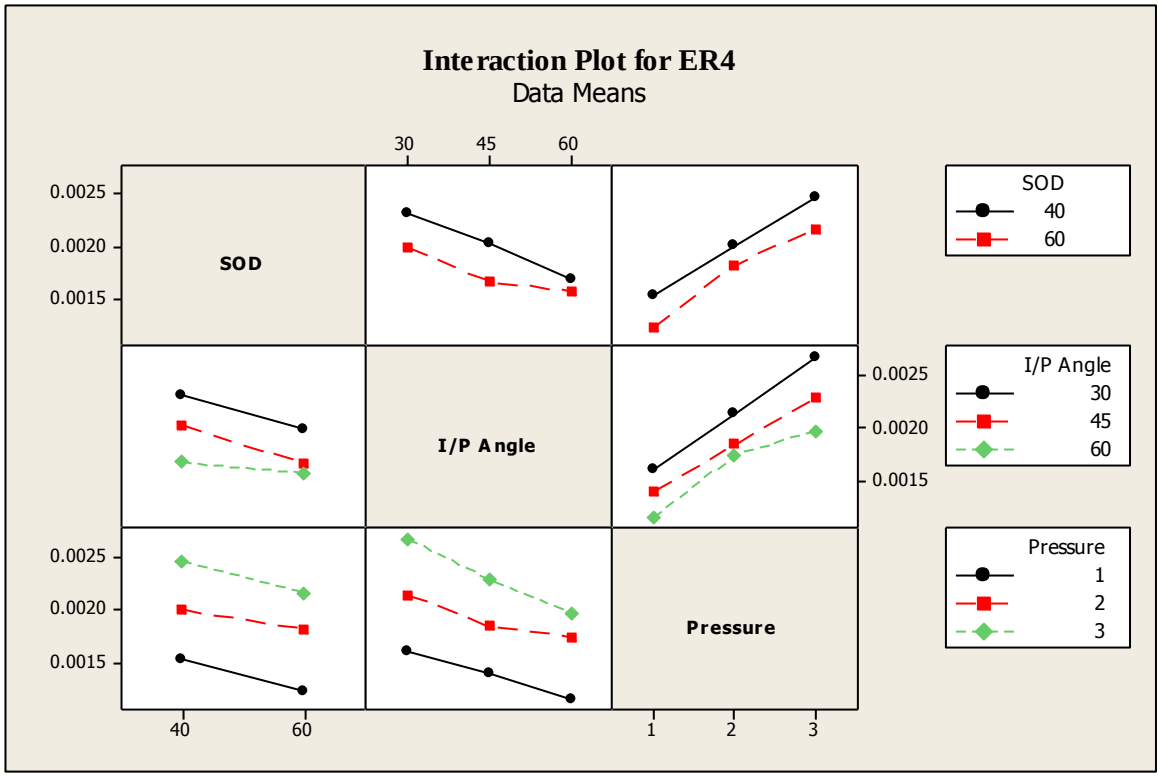

Fig.4.9- Interaction plot (For sample 4)

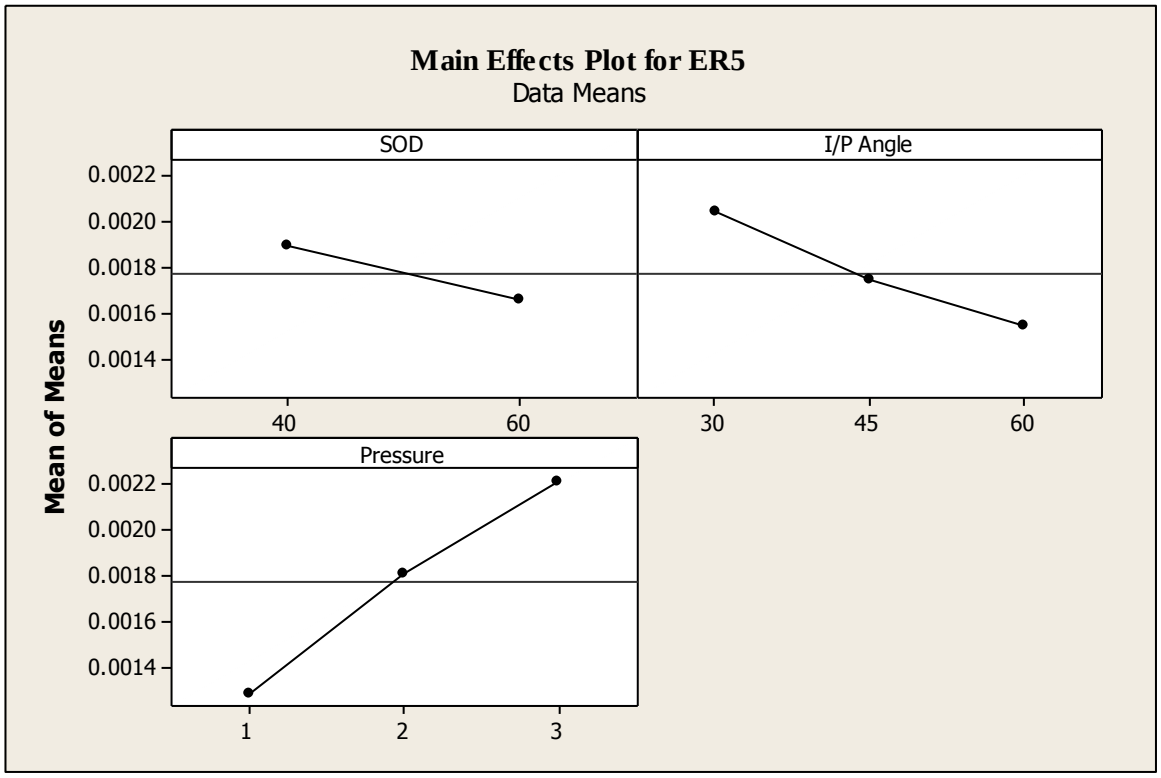

Fig. 4.10 - Effect of control factors on erosion rate. (For sample 5)

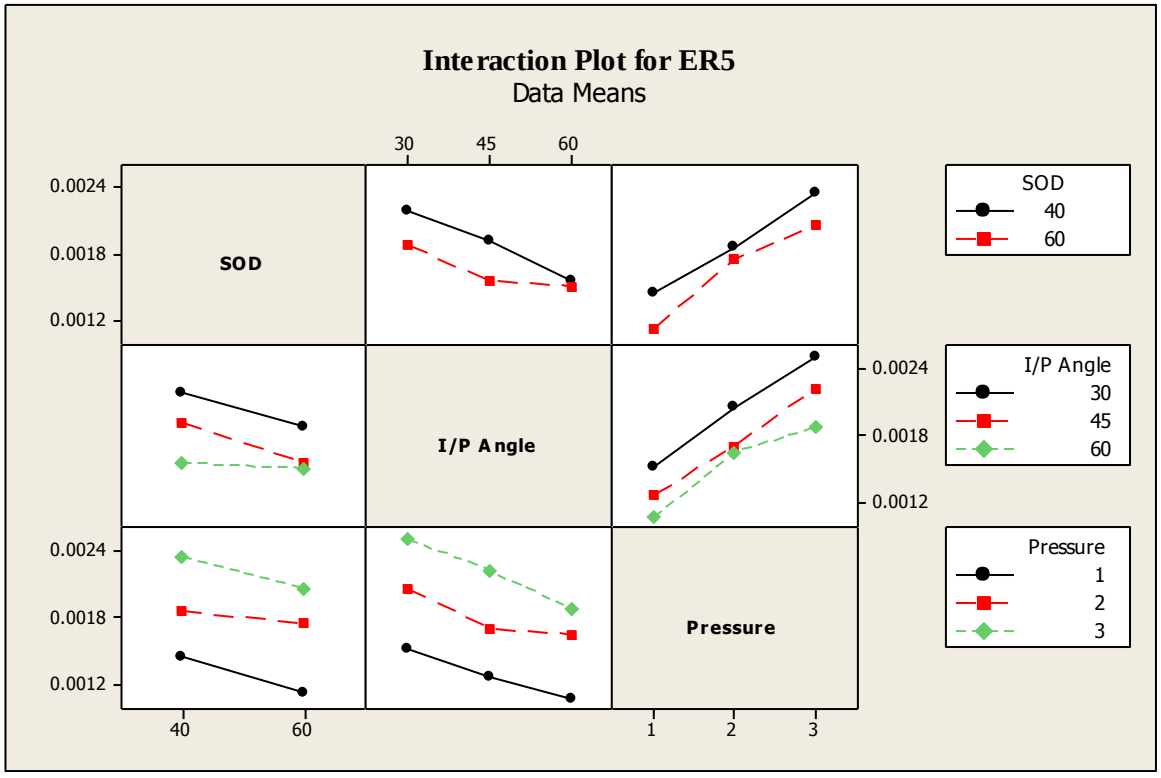

Fig.4.11- Interaction plot (For sample 5)

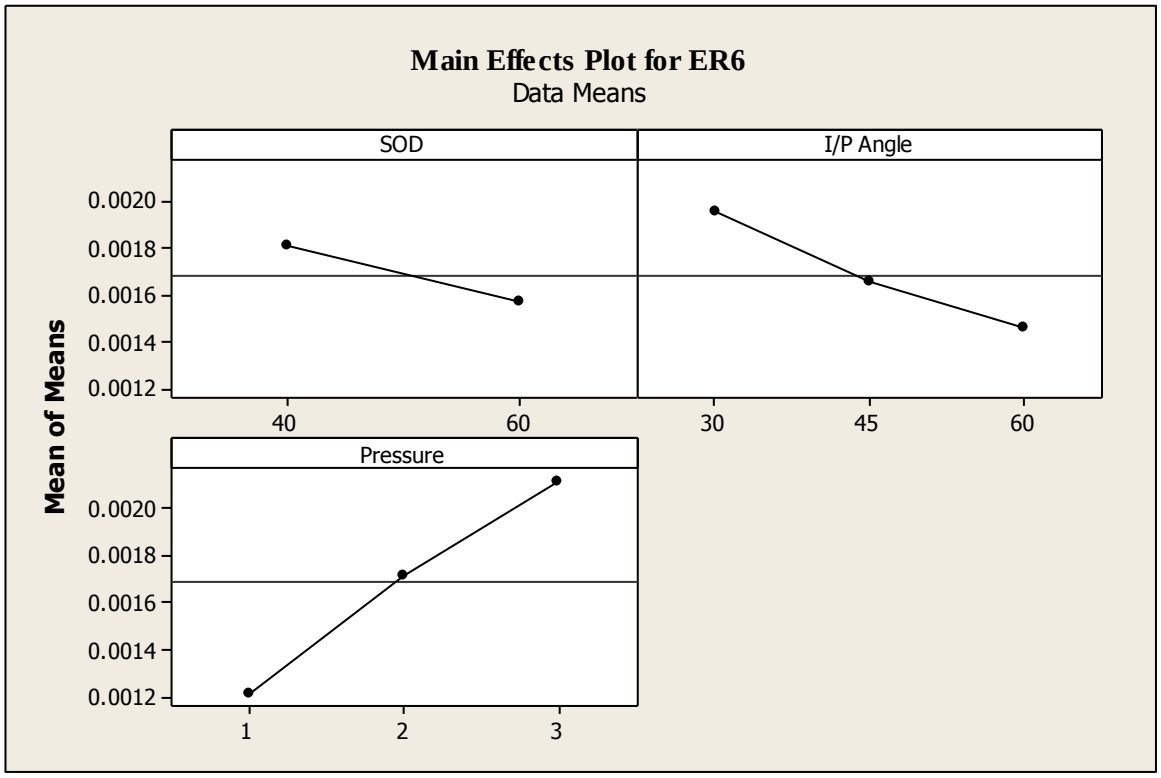

Fig 4.12- Effect of control factors on erosion rate. (For sample 6)

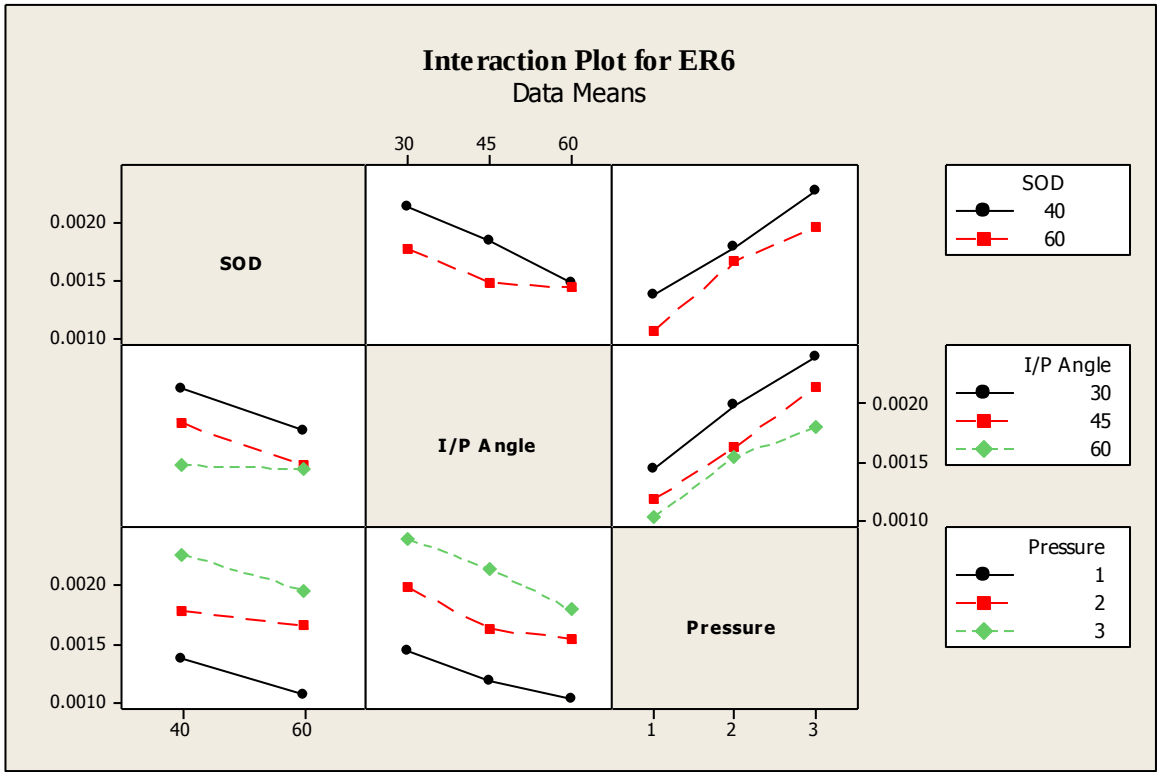

Fig 4.13- Interaction plot (For sample 6)

Level	SOD	I/P Angle	Pressure
1	0.002286	0.002430	0.001575
2	0.002017	0.002130	0.002185
3		0.001893	0.002693
Delta	0.000269	0.000537	0.001118
Rank	3	2	1

Sample 1

Level	SOD	I/P Angle	Pressure
1	0.002123	0.002238	0.001482
2	0.001856	0.002007	0.002005
3		0.001723	0.002982
Delta	0.000268	0.000515	0.001000
Rank	3	2	1

Sample 2

Level	SOD	I/P Angle	Pressure
1	0.002057	0.002177	0.001417
2	0.001780	0.001898	0.001940
3		0.001680	0.002398
Delta	0.000277	0.000497	0.000982
Rank	3	2	1

Sample 3

Level	SOD	I/P Angle	Pressure
1	0.002006	0.002145	0.001388
2	0.001792	0.001848	0.001917
3		0.001628	0.002317
Delta	0.000263	0.000517	0.000928
Rank	3	2	1

Sample 4

Level	SOD	I/P Angle	Pressure
1	0.001890	0.002035	0.001290
2	0.001650	0.001738	0.001810
3		0.001537	0.002210
Delta	0.000240	0.000498	0.000920
Rank	3	2	1

Sample 5

Level	SOD	I/P Angle	Pressure
1	0.001810	0.001950	0.001220
2	0.001563	0.001653	0.000722
3		0.001457	0.002118
Delta	0.000247	0.000493	0.000898
Rank	3	2	1

Sample 6

Table 4.1- Response table for means for different samples

4.5.1 STATISTICAL ANALYSIS

SAMPLE NUMBER	S	R-Sq	R-Sq (adj)
1	0.00007078	99.6%	98.3%
2	0.00006407	99.6%	98.4%
3	0.00006916	99.5%	98.0%
4	0.00007047	99.5%	97.8%
5	0.0001119	98.7%	94.4%
6	0.0001189	98.5%	93.5%

Table 4.2: Statistical Analysis of different sample

The experiment has been done keeping in view that the result holds good and fits in normal distribution. The statistics used are S, R-Sq, R-Sq (adj.) and the corresponding values of goodness of fit is shown in table x for all the samples.

4.6 MICROSTRUCTURAL INVESTIGATION

Fig. 4.14 shows the eroded surface after the erosion test for different samples. It can be seen that impact angles affect the morphologies of the eroded scars substantially. In the erosion mechanism of the spheroidal graphite at the surface deforms gradually, lips are produced in the direction of the blast, and they extend, and finally drop off. This process of growth, extension, and dropping off is repeated, but life spans are different depending on the material**.**

The basic mechanism of the erosion damage is at first the plastic transformation near the surface owing to the impacts. The wear damage proceeds with the growth and breaking off of ridges. The size of ridges depends on structure and mechanical properties of material, and this causes differences in erosion rates of various structures.

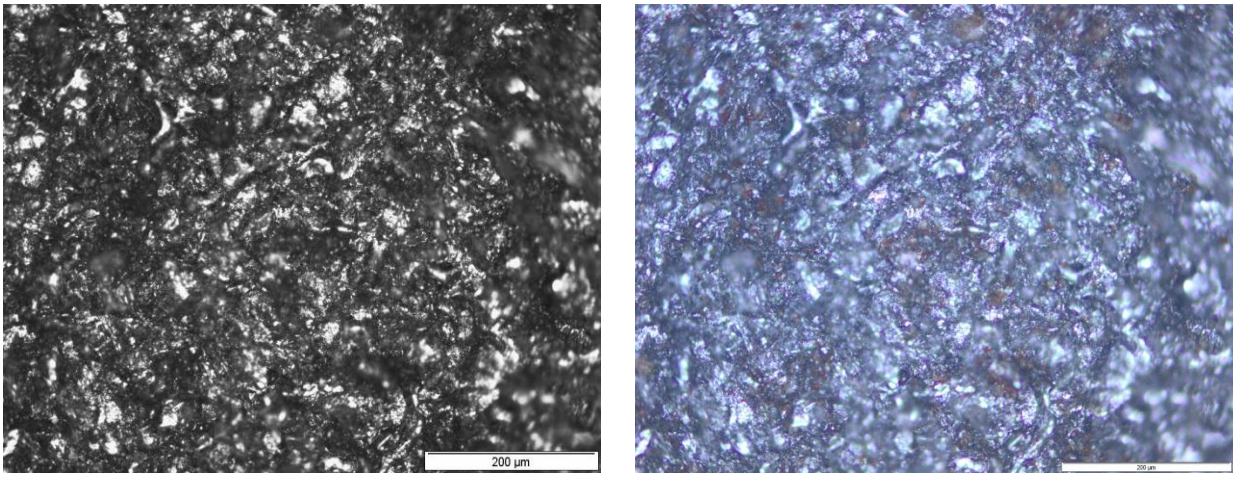

Fig. (a)- Eroded Surface of SG iron sample 1

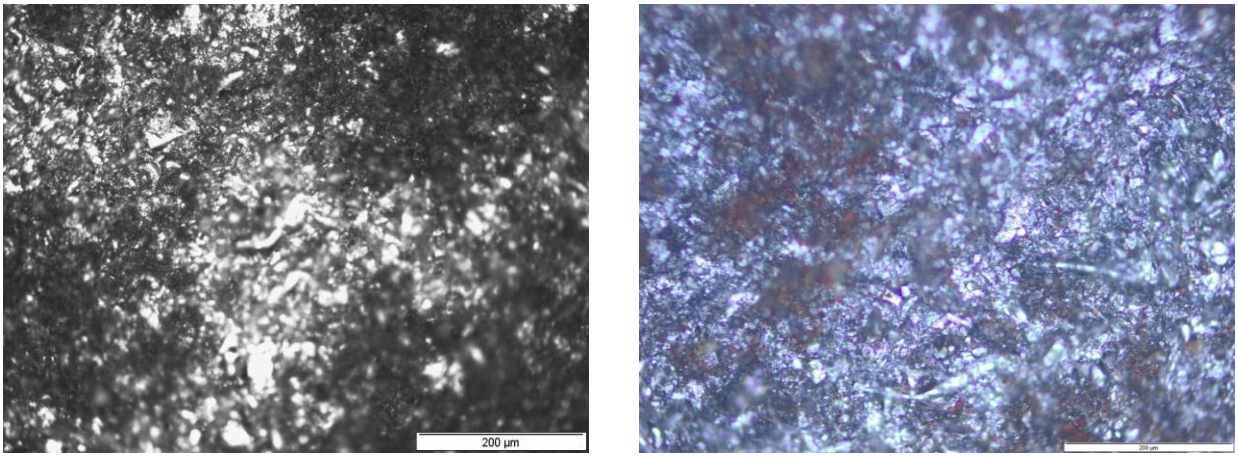

Fig. (b)- Eroded Surface of SG iron sample 2

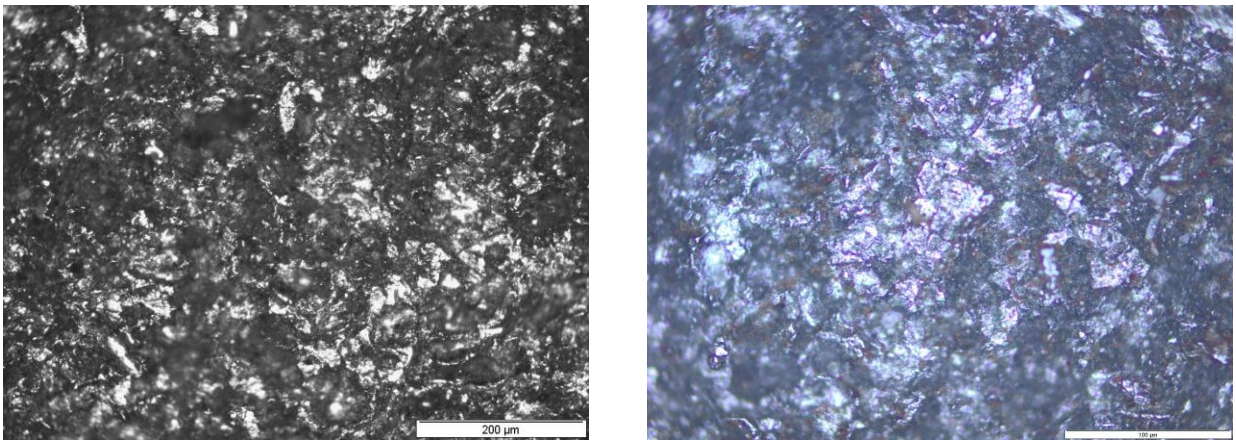

Fig. (c)- Eroded Surface of SG iron sample 3

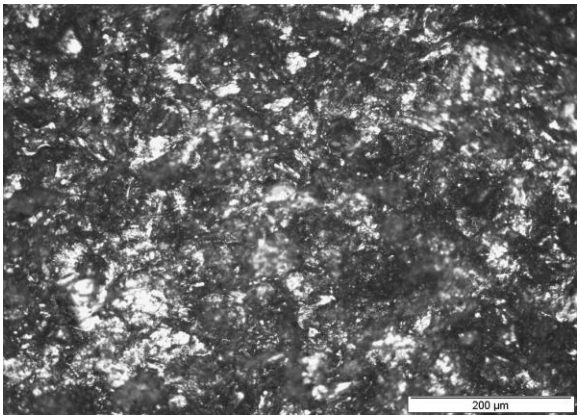

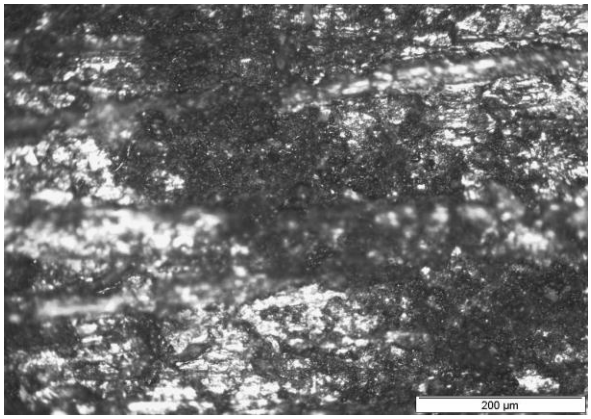

Fig. (d)-Eroded Surface of SG iron sample 4

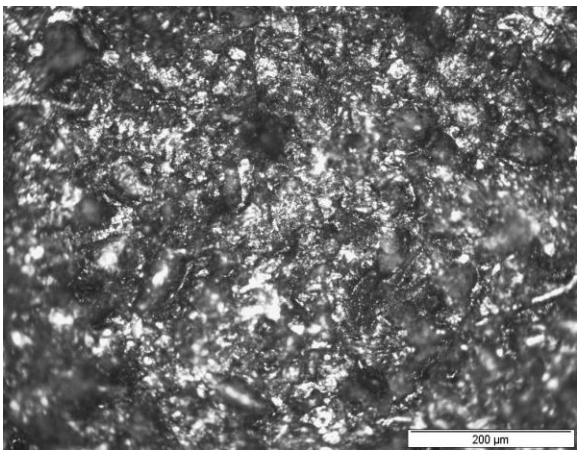

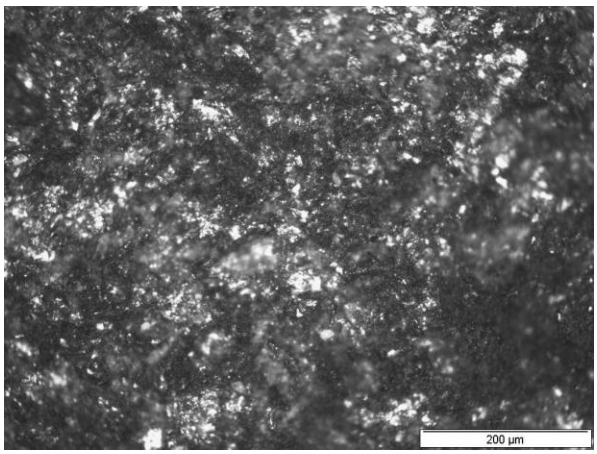

(e) **(f)**

Fig.4.14 Eroded Surface of SG iron (a) sample 1, (b) sample 2, (c) sample 3, (d) sample 4, (e) sample 5, (f) sample 6

As a result of the foregoing findings, a general conception of the effect of the impact angle on the erosion rate and erosion mechanisms of a ductile material subjected to slurry erosion can be postulated. With the change of the impact angle from 30˚ up to 60◦ two different regions can be noticed, namely, a region of small impact angles $\theta \leq 45^\circ$, and finally a region of high impact angles $45^\circ \leq \theta \leq 60^\circ$.

In the first region, $\theta \leq 45^\circ$, the normal component of the impact force is too small compared to the tangential one. This means that the normal component of the impact energy imparted by the impacting particles to the target material is small and be expected to be less than the resilience, i.e. the elastic strain energy, of the target material. Therefore, the impacting particles do not penetrate into the target surface and the elastic strain energy may lead to rebound

of the impacting particles. As a result of the large tangential component of the impacting force which is accompanied with small normal component the erodent particles may roll or scratch the target surface [84]. The displaced materials due to shallow ploughing at the sides and in front of the wear scars are limited and detached due to repeated impacts. Therefore, the first region is distinguished with shallow long scratches and small rate of erosion. Low impact angle is associated with high erosion rate, while high impact angle is associated with low erosion rate.

CHAPTER 5

CONCLUSION

- Conclusion
- Future scope of work

CONCLUSION

- It is observed that hardness of eroded surface increases after erosion test due to work hardening of material.
- The surface hardness of sample before erosion test are varies from 125HV20 to 215HV20 and after erosion test are varies from 175HV20 to 295HV20.
- Nodular cast iron (SG iron) shows the highest wear resistance probably due to its graphite morphology which controls crack propagation and thermal conductivity.
- Particle erosion characteristics of these SG iron samples can be successfully analyzed using the Taguchi experimental design scheme. Taguchi method offers a simple, organized and efficient methodology for the optimization of the control factors.
- The results indicate that pressure, impingement angle and stand of distance are the significant factors in a declining sequence affecting the erosion wear rate. Although the effect of stand of distance is less compared with other factor and interaction plot not cross each other it means pressure, impact angle and stand of distance not depends on each other. An optimal parameter combination is determined, which leads to minimization of material loss due to erosion.

FUTURE SCOPE OF WORK

Spheroidal graphite Iron's application has increased tremendously in many industrial areas. It is increasingly the material of choice of designers and engineers because of their cost effective performance. It has started to replace steel in some structural applications. It has also found its marvelous applications in automobile sector which includes crankshafts, disc-brake calipers, axle housings, etc. It is also used to manufacture spun pipes, pump bodies, rock drillers, etc. For all these applications, we want to take into consideration various other mechanical properties like impact resistance, fracture toughness, creep resistance, noise reduction and energy saving properties, etc. So in future, we can measure the above mentioned mechanical properties to optimally select a material for its specific application. Evaluation of thermal stability of these SG iron is to be evaluated to find high temperature applications. In future Sliding wear, abrasion wear behaviour under different operating conditions can be investigated to identify suitable application areas.

REFERENCES

[1] J. Jault, Fontes à graphite sphéroïdal: propriétés d'utilisation, Techniques de l'ingénieur (M 4 610) (2007) 1–25.

[2] Nicola Bonora, AndrewRuggiero, Micromechanical modeling of ductile cast iron incorporating damage, Part 1: Ferritic ductile cast iron, international Journal of Solids and Structures 42 (2006) 1401–1424.

[3] J.S.L. Magalhaes, C. Sa, Experimental observations of contact fatigue crack mechanisms for austempered ductile iron (ADI) discs, Wear 246 (1–2) (2000) 134–148.

[4] M. Hatate, T. Shoita, N. Takahashi, K. Shimizu, Influence of graphite shapes on wear characteristics of austempered cast iron, Wear 251 (2001) 885–889.

[5] R.C. Dommarco, J.D. Salvande, Contact fatigue resistance of austempered and partially chilled ductile irons, Wear 254 (2003) 230–236.

[6] L. Collini, Micromechanical modeling of the elasto-plastic behavior of heterogeneous nodular cast iron, doctarat en genie industrilel, Universita'Degli Studi di Parma, 2004.

[7] Forrest R D. Austempered Ductile Iron for Both Strength and Toughness. Machine Design. 1985. 57(22), 95.

[8] Crane FAA. Charls J A. Selection and Use of Engineering Materials. London, Butterworth. 1984.

[9] Dorazil E. Barta B. Munsterova E. High Strength Bainitic Ductile Cast Iron. AFS International Cast Metals Journal. 1982. 7(2): 52.

[10] ASM. Metals Handbook. 8th ed. Metals Park, ASM. 1974

[11] Jolley G. Gilbert G N J. Segragation in Nodular Iron and Its Influence on Mechanical Properties. The British Foundryman. 1967. 60(3), 79.

[12]John R. Keough, PE Kathy L. Hayrynen, PhD Applied Process Inc. Technologies Div. Livonia, Michigan, USA

[13] Gahr KH. Wear by hard particles. Tribol Int 1998; 31(10):587–96.

[14] Robinowicz ED. Friction and wear of materials. New York: Wiley; 1965. p. 18.

[15] Islam MA, Haseeb ASMA, Kurny ASW. Study of as cast and heat treated spheroidal graphite cast iron under dry sliding conditions. Wear 2000; 244:15–9.

[16] Sahin Y. Optimal testing parameters on the wear behaviour of various steels. Mater Des 2006; 27:455–60.

[17] Fernandez JEsteban, Fernandez MR, Diaz RV, Navarro RT. Abrasive wear analysis using factorial experiment design. Wear 2000;255:38–43.

[18] Spuzic S, Zee SM, Abhay K, Ghomasch R, Reid I. Fractional design of experiments applied to a wear simulation. Wear 1997; 212:131–9.

[19] Roy KR. A primer on the Taguchi method, Competitive manufacturing series. New York, USA: Van Nonstrand Reinhold; 1990.

[20] Cueva G, Sinatora A, Guesser WL, Tschiptsch AP. Wear resistance of cast iron used in brake disc rotors. Wear 2003; 255:1256–60.

[21] Charpman BJ, Manniean G. Titanium-bearing cast iron for automotive braking apparatus. Foundary Trade J. 1982; 25:232.

[22] Nili Ahmadabadi M, M Ghasemi H, Osia M. Effects of successive austempering on the tribological behaviour of ductile cast iron. Wear 1999; 231:293–300.

[23] Hatate M, Shiota T, Takahashi N, Shimizu K. Influences of graphites shapes on wear characteristics of austempered cast iron. Wear 2001; 251:885–900.

[24] Domarco RC, Salvande JD. Contact fatigue resistance austempered and partially chilled ductile irons. Wear 2003; 254:230–6.

[25] Haseeb ASMA, Aminul Islam MD, Bepari Mohar Ali. Tribological behaviour of quenched and tempered, and austempered ductile iron at the same hardness level. Wear 2000; 244:15–9.

[26] Zimba J, Samandi M, Yu D, Chandra T, Navara E, Simbi DJ. Unlubricated sliding wear performance of unalloyed austempered ductile iron under high contact stresses. Mater Des 2004; 25(5): 431–8.

[27] Bosnjak B, Verlinden B, Radulovic B. Dry sliding wear of low alloyed austempered ductile iron. Mater Sci Technol 2003; 19:650–6.

[28] Luo Q, Xie J, Song Y. Effects of microstructures on the abrasive wear behaviour of spheroidal cast iron. Wear 1995; 184:19–23.

[29] Hisakado T, Suda H, Trukui T. Effects of dislodgement and size of abrasive grains on abrasive wear. Wear 1992; 155:297–307.

[30] Rebasa N, Dommarco R, Sikora J. Wear resistance of high nodule count ductile iron. Wear 2002; 253:55–861.

[31] Jeng M-C. Abrasive wear of bainitic nodular cast iron. J Mater Sci 1993; 28:6555–61.

[32] Ceccarelli BA, Dommarco RC, Martinez RA, Gamba MRMartinez. Abrasion and impact properties of partially chilled ductile iron. Wear 2004; 256:49–55.

[33] Rajasekaran S , Vijayalakshmi G A, Pai –neural networks, fuzzy logic and genetic algorithm –synthesis and application--Prentice Hall of India Pvt.
Ltd., New Delhi (2003)

[34] ASM specialty hand book, cast iron, J.R.Davis, 1st edition, ASM international, Ohio, 356-392(1996).

[35] "Meehanite ADI- Guidelines for Designing and Machining Meehanite Austempered Ductile Iron Castings", Meehanite Metal Corporation publication B88/4/88.

[36]Chatterley, T.C., Murrell, P., "ADI Crankshafts-An Appraisal of Their Production Potential", SAE 980686, SAE International Congress & Exposition, Detroit, Michigan, USA February 1998.

[37] John R. Keough, PE, Kathy L. Hayrynen, PhD Automotive Applications of Austempered Ductile Iron (ADI): A Critical Review, Copyright © 2000 Society of Automotive Engineers.

[38] W.T. Cheng, H.C. Li and C.N. Huang "Simulation and optimization of silicon thermal CVD through CFD integrating Taguchi method" Chemical Engineering Journal, Volume 137, Issue 3, April 2008, Pp 603-613.

[39] S.Basavarajappay and G.Chandramohan Wear Studies on Metal Matrix Composites: a Taguchi Approach, J. Mater. Sci. Technol., Vol.21 No.6, 2005.

[40] Bala Murugan Gopalsamy, Biswanath Mondal and Sukamal Ghosh, "Taguchi method and ANOVA: An approach for process parameters optimization of hard machining while machining hardened steel".Journal of Scientific and Industrial Research, Vol. ^8, August 2009, pp. 686-695.

[41] Sagar Jagtap and Uday A. Dabade, "Analysis of process parameters during machining of difficult to cut material using EDM process", M. Tech. dissertation report, Walchand College of Engineering, Sangli, 11 July, 2010.

[42] Uday A. Dabade, S. S. Joshi and N. Ramakrishnan, "Analysis of surface roughness and chip cross sectional area while machining with self-propelled round insert milling cutter"

[43] Madhav S. Phadke, "Quality engineering using Rombust design", Prentice hall, Englewood Cliff, New Jersey, ISBN 0-13-745167-9.

[44] Holm R., "The frictional force over the real area of Contact", Wiss. Vereoff. Siemens Werken, Volume17, No.4, (1938): p. 38-42.

[45] Ashby M. F. and Lim S. C., 'Wear - mechanism maps.' Scripta Metallurgical et Materialia.Volume24, (1990): p. 805-810.

[46] Wang Y., lei T.C. and Gao C.Q., 'Influence of isothermal hardening on the sliding wear behaviour of 52100 bearing steel. Tribology International. Volume 23, No.1, (1990): p.47-63.

[47] Soda N., 'Wear of some F.F.C metals during unlubricated sliding part-1.Effects of load, velocity and atmospheric pressure on wear'. Wear. Volume33, (1975):p. 1-16.

[48] Burwell J.T. and Strang C.D, 'Metallic wear', Proc. Soc (London), 212A May 1953, p. 470-477.

[49] Burwell J .T. 'Survey of possible wear mechanisms.' Wear. Volume1, (1957/58): p.119-141.

[50] K.H.Zumgahr, 'Microstructure and wear of materials' Elsevier, Amsterdam, 1987.

[51] P.L.Ko, "Metallic wear-a review with special references to vibration-induced wear in power plant components." Tribology International Volume 20, No. 1, (April 1987): p.66-78.

[52] Eyre L.S., "Wear Characteristics of metals." Tribology International (October 1976):p. 203-212.

[53] Dowson, "Wear oh where." International Conference on wear of Materials, Vancouver Canada, April 14-18, 1985.

[54] Peterson.M. B, "Advanced in tribo-materials I Achievements in Tribology", Amer, Soc, Mech. Eng., Volume1, New York, 1990, pp. 91-109.

[55] Blau J. "Fifty years of research on the wear of metals." Tribology International Volume 30, No.5, (1997): p. 321-331.

[56] Rao V and Rao H, 'C++ Neural Networks and Fuzzy Systems' BPB Publication 2000.

[57] I.M. Hutchings, R.E. Winter, Particles erosion of ductile metals: a mechanism of material removal, Wear 27 (1974) 121–128.

[58] I.M. Hutchings, Mechanism of the Erosion of Metals by Solid Particles, ASTM STP664, 1979, p. 59–76.

[59] I. Hussainova, Microstructure and erosive wear in ceramic-based composites, Wear 258 (2005) 357–365.

[60] D.W. Wheeler, R.J.K. Wood, Erosion of hard surface coatings for use in offshore gate valves, Wear 258 (2005) 526–536.

[61] I. Finnie, Erosion of surfaces by solid particles, Wear 3 (1960) 87–103.

[62] J.G.A. Bitter, A study of erosion phenomena. Part I, Wear 6 (1963) 5–21.

[63] J.G.A. Bitter, A study of erosion phenomena. Part II, Wear 6 (1963) 169.

[64] J.H. Neilson, A. Gilchrist, Wear 11 (1968) 111.

[65] G.P. Tilly, Erosion caused airborne particles, Wear 14 (1969) 63–79.

[66] G.P. Tilly, Sand erosion of metals and plastics: a brief review, Wear 14 (1969) 241–248.

[67] G.P. Tilly, W. Sage, The interaction of particle and material behaviour in erosion processes, Wear 16 (1970) 447–465.

[68] G.P. Tilly, A two stage mechanism of ductile erosion, Wear 23 (1973) 87–96.

[69] Jorge L. Garin[a1], Rodolfo L. Mannheim and Marco A. Soto

[70] W.A. Glaeser, A. Dow, Mechanisms of erosion in slurry pipelines, in: Proceedings of the second international conference on slurry transportation, Las Vegas, NV: March 2–4, 1977, pp. 136–140.

[71] J.A. Laitone, Erosion prediction near a stagnation point resulting from aerodynamically entrained solid particles, Journal of Aircraft 16 (12) (1979) 809–814.

[72] M.M. Salama, E.S. Venkatesh, Evaluation of erosion velocity limitations of offshore gas wells, in: 15th Annual OTC, Houston, TX: May 2-5, OTC no. 4485, 1983.

[73] A.T. Bourgoyne, Experimental study of erosion in diverter systems due to sand production, in: Presented at the SPE/IADC Drilling Conference SPE/IADC 18716 New Orleans, LA, 1989, pp. 807–816.

[74] D.P. Chase, E.F. Rybicki, J.R. Shadley, A model for the effect of velocity on erosion of N80 steel tubing due to the normal impingement of solid particles, Transactions ASME Journal of Energy Resources Technology 114 (1992) 54–64.

[75] B.S. McLaury, A model to predict solid particle erosion in oil field geometries. MS thesis, The University of Tulsa, (1993).

[76] S.J. Svedeman, K.E. Arnold, Criteria for sizing Multiphase flow lines for erosive/ corrosive services, Paper presented at the 1993 SPE conference, Houston SPE 265 (1993) 69.

[77] K Jordan, Erosion in multiphase production of oil and gas, Corrosion 98, Paper no. 58, NACE International Annual Conference, San Antonio. (1998).

[78] S.A. Shirazi, B.S. McLaury, Erosion modelling of elbows in multiphase flow. In: Proceedings of 2000 ASME fluids engineering summer meeting, June 11–15, Boston, MA: Paper no. FEDSM2000-11251. (2000).

[79] C.G. Ferreira, D. Ciampini, M. Papini, The effect of inter-particle collisions in erosive streams on the distribution of energy flux incident to a flat surface, Tribology International 37 (2004) 791–807.

[80] M. Papini, D. Ciampini, T. Krajac, J.K. Spelt, Computer modelling of interference effects in erosion testing: effect of plume shape, Wear 255 (1–6) (2003) 85–97.

[81] Finnie I. Wear 1995; 186/187:1–20.

[82] Oka YI, Ohnogi H, Hosokawa T, Matsumura M. Wear 1997;203/ 204:573–9.

[83] Shin YW, Sargent GA, Contrad H. Metall Trans 1987; A18: 437–49.

[84] K.C. Chen, J.L. He, W.H. Huang, T.T. Yeh, Study on the solid–liquid erosion resistance of ion-nitrided metal, Wear 252 (2002) 580–585.